

# Dbf4-dependent kinase and the Rtt107 scaffold promote Mus81-Mms4 resolvase activation during mitosis

Lissa N Princz<sup>1</sup>, Philipp Wild<sup>2</sup>, Julia Bittmann<sup>1</sup>, F Javier Aguado<sup>3</sup>, Miguel G Blanco<sup>3</sup> , Joao Matos<sup>2</sup> & Boris Pfander<sup>1,\*</sup> 

## Abstract

DNA repair by homologous recombination is under stringent cell cycle control. This includes the last step of the reaction, disentanglement of DNA joint molecules (JMs). Previous work has established that JM resolving nucleases are activated specifically at the onset of mitosis. In case of budding yeast Mus81-Mms4, this cell cycle stage-specific activation is known to depend on phosphorylation by CDK and Cdc5 kinases. Here, we show that a third cell cycle kinase, Cdc7-Dbf4 (DDK), targets Mus81-Mms4 in conjunction with Cdc5—both kinases bind to as well as phosphorylate Mus81-Mms4 in an interdependent manner. Moreover, DDK-mediated phosphorylation of Mms4 is strictly required for Mus81 activation in mitosis, establishing DDK as a novel regulator of homologous recombination. The scaffold protein Rtt107, which binds the Mus81-Mms4 complex, interacts with Cdc7 and thereby targets DDK and Cdc5 to the complex enabling full Mus81 activation. Therefore, Mus81 activation in mitosis involves at least three cell cycle kinases, CDK, Cdc5 and DDK. Furthermore, tethering of the kinases in a stable complex with Mus81 is critical for efficient JM resolution.

**Keywords** cell cycle; genome stability; homologous recombination; joint molecule resolution; post-translational modification

**Subject Categories** Cell Cycle; DNA Replication, Repair & Recombination

**DOI** 10.15252/embj.201694831 | Received 22 May 2016 | Revised 15 December 2016 | Accepted 19 December 2016 | Published online 18 January 2017

**The EMBO Journal (2017) 36: 664–678**

## Introduction

Many DNA transactions are under cell cycle control to adjust them to cell cycle phase-specific features of chromosomes (Branzei & Foiani, 2008). Homologous recombination (HR) is cell cycle-regulated at several steps including the first, DNA end resection, and the

last, JM removal (Heyer *et al*, 2010; Ferretti *et al*, 2013; Mathiasen & Lisby, 2014; Matos & West, 2014). Given that JMs provide stable linkages between sister chromatids, they will interfere with chromosome segregation and therefore need to be disentangled before sister chromatid separation during mitosis. Accordingly, JM resolvases, such as budding yeast Mus81-Mms4 (Interthal & Heyer, 2000; Schwartz *et al*, 2012) or Yen1 (Ip *et al*, 2008), become activated during mitosis (Matos *et al*, 2011, 2013; Gallo-Fernández *et al*, 2012; Szakal & Branzei, 2013; Blanco *et al*, 2014; Eissler *et al*, 2014). In contrast, the alternative JM removal pathway, JM dissolution by the Sgs1-Top3-Rmi1 complex, is thought to be constantly active throughout the cell cycle (Mankouri *et al*, 2013; Bizard & Hickson, 2014). The activation of JM resolvases in mitosis therefore leads to a shift in the balance between JM removal pathways, with dissolution being preferred outside of mitosis, but JM resolution becoming increasingly important in mitosis (Matos *et al*, 2011, 2013; Gallo-Fernández *et al*, 2012; Dehé *et al*, 2013; Saugar *et al*, 2013; Szakal & Branzei, 2013; Wyatt *et al*, 2013). It has been hypothesized that JM resolvases are downregulated at cell cycle stages other than mitosis in order to counteract crossover-induced loss of heterozygosity or to prevent over-active resolvases from interfering with S phase by, for example, cleaving stalled replication forks (Gallo-Fernández *et al*, 2012; Szakal & Branzei, 2013; Blanco *et al*, 2014).

Budding yeast Mus81-Mms4 has previously been shown to be targeted by two cell cycle kinases, cyclin-dependent kinase Cdc28 (CDK) and the yeast polo-kinase Cdc5 (Matos *et al*, 2011, 2013; Gallo-Fernández *et al*, 2012; Szakal & Branzei, 2013). The corresponding Mms4 phosphorylation events were shown to correlate with and to be required for activation of Mus81-Mms4 in mitosis. In 2014, we showed that in mitosis Mus81-Mms4 also forms a complex with Slx4-Slx1 and the scaffold proteins Dpb11 and Rtt107 (Gritenaite *et al*, 2014). Interestingly, mass spectrometric analysis of this complex (Gritenaite *et al*, 2014) revealed that Cdc5 and a third cell cycle kinase Dbf4-Cdc7 (Dbf4-dependent kinase, DDK) are also a stable part of this protein assembly (see Appendix Fig S1A). Here,

<sup>1</sup> Max Planck Institute of Biochemistry, DNA Replication and Genome Integrity, Martinsried, Germany

<sup>2</sup> Institute of Biochemistry, Eidgenössische Technische Hochschule, Zürich, Switzerland

<sup>3</sup> Department of Biochemistry and Molecular Biology, Center for Research in Molecular Medicine and Chronic Diseases, Universidade de Santiago de Compostela, Santiago de Compostela, Spain

\*Corresponding author. Tel: +49 89 85783050; Fax: +49 89 85783022; E-mail: bpfander@biochem.mpg.de

we investigate the role of DDK in Mus81-Mms4 regulation and find that DDK can phosphorylate Mms4 and that DDK and Cdc5 target Mus81-Mms4 in an interdependent manner. Moreover, we show that Rtt107 promotes the association of both kinases with the Mus81-Mms4 complex. The DDK-dependent regulation of Mus81-Mms4 is critical for Mus81 activity thus revealing DDK as a novel regulator of homologous recombination.

## Results

### Mus81-Mms4 is a DDK phosphorylation target

The cell cycle regulation of JM resolution by Mus81-Mms4 is intricate and involves phosphorylation by the cell cycle kinases CDK

and Cdc5 (Matos *et al.*, 2011, 2013; Gallo-Fernández *et al.*, 2012; Szakal & Branzei, 2013) as well as complex formation with the scaffold proteins Dpb11, Slx4 and Rtt107 (Gritenaite *et al.*, 2014). To study this protein complex, we performed an analysis of Mms4<sup>3FLAG</sup> interactors in mitosis by SILAC-based quantitative mass spectrometry (Gritenaite *et al.*, 2014) and found in addition to Dpb11, Slx4, Rtt107 and Cdc5, also Cdc7 and Dbf4 as specific interactors of Mms4 (Appendix Fig S1A). We verified that Cdc7 binds to Mus81-Mms4 in an Mms4<sup>3FLAG</sup> pull down from mitotic cells analysed by Western blots (Fig 1A). The fact that Mus81-Mms4 binds to DDK suggested that it might be involved in the phosphorylation cascade that occurs on Mms4 and controls Mus81 activity in mitosis. Accordingly, we found that purified DDK was able to phosphorylate both subunits of purified Mus81-Mms4 *in vitro* (Fig 1B, lane 3). When we furthermore compared the DDK-dependent

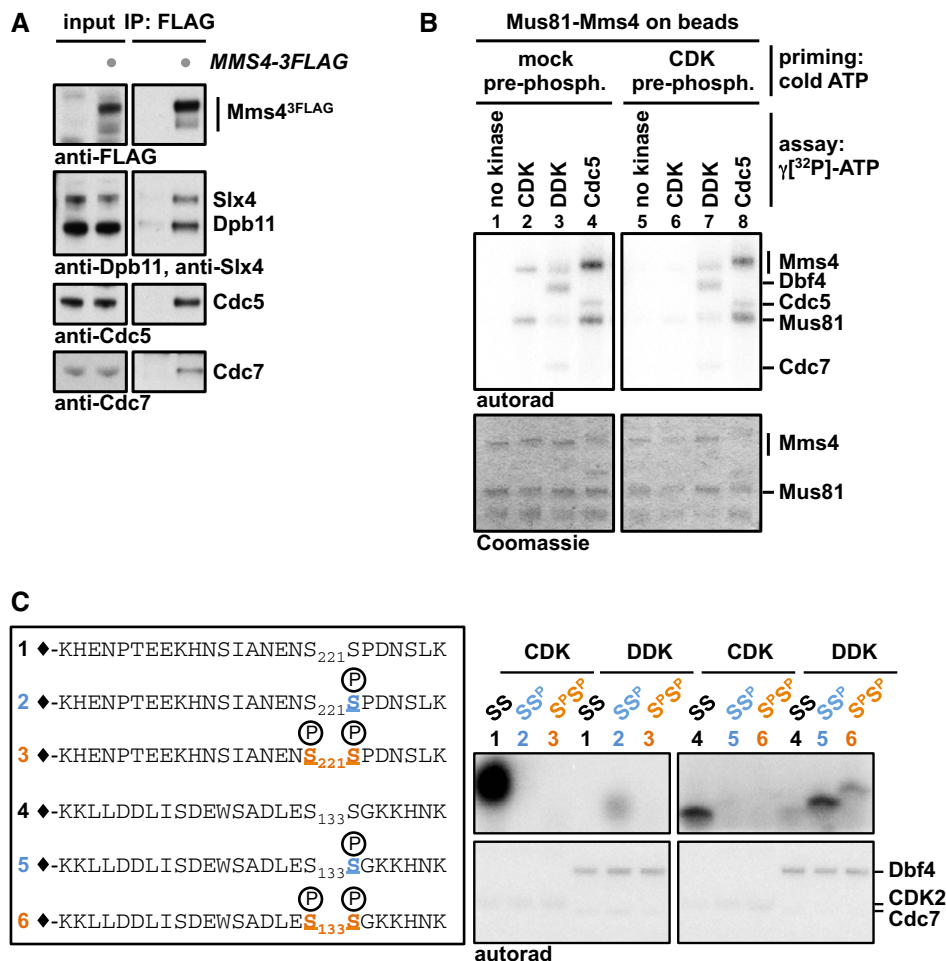


**Figure 1. Dbf4-dependent kinase (DDK) binds to the Mus81-Mms4 complex in mitosis and can phosphorylate Mms4 at (S/T)(S/T) motifs.**

A Cdc7 and Cdc5 are specifically enriched in Mms4<sup>3FLAG</sup> co-IPs from cells arrested in mitosis (with nocodazole). Under the same conditions, Mus81-Mms4 associates with scaffold proteins such as Dpb11 and Slx4 (Appendix Fig S1A and Gritenaite *et al.*, 2014).

B DDK can phosphorylate Mus81-Mms4 *in vitro*. Purified, immobilized Mus81-Mms4 is incubated in an *in vitro* kinase assay with purified CDK2/cycA<sup>N170</sup> (a model CDK), DDK or Cdc5 (lanes 1–4). Additionally, Mus81-Mms4 is incubated with respective kinases after a non-radioactive priming step with CDK (lanes 5–8).

C DDK phosphorylates Mms4 peptides at (S/T)(S/T) motifs and is enhanced by priming phosphorylation. Mms4 peptides including (S/T)(S/T) motifs (221/222; 133/134) were synthesized in different phosphorylation states (depicted in left panel) and incubated in an *in vitro* kinase assay with either CDK or DDK. CDK targets unphosphorylated Mms4 peptides 1 and (to a weaker extent) 4 consistent with its substrate specificity (Mok *et al.*, 2010), while DDK primarily targets Mms4 peptides 2 and 5, which harbour a priming phosphorylation at the C-terminal (S/T) site (see Appendix Fig S1B for in-gel running behaviour of peptides).

phosphorylation signal to Mms4 phosphorylation by CDK and Cdc5 (Fig 1B, lanes 2–4), we observed different degrees of phosphorylation shifts indicating that the three kinases phosphorylate Mms4 at distinct sites and/or to different degrees. DDK target sites on other proteins have been studied in detail, and in several cases, DDK was found to target (S/T)(S/T) motifs, where phosphorylation was stimulated by a priming phosphorylation usually on the second (S/T) (Masai *et al*, 2006; Montagnoli *et al*, 2006; Randell *et al*, 2010; Lyons *et al*, 2013). Intriguingly, Mms4 contains 15 of these motifs and we therefore tested whether these could be targeted by DDK and would depend on priming phosphorylation. We therefore turned to a peptide-based assay where Mms4 phosphorylation states are precisely defined. To this end, we synthesized peptides corresponding to two (S/T)(S/T) motifs of Mms4. We chose two representative motifs: S222, as it harbours a minimal CDK consensus motif (S/T)P, and S134, as it contains a non-(S/T)P consensus for CDK [(S/T)X(K/R)(K/R) (Suzuki *et al*, 2015)]. For each of these motifs, we generated peptides in three different phosphorylation states: non-phosphorylated, phosphorylated at the second serine and doubly phosphorylated (Fig 1C and Appendix Fig S1B). When using such peptides as substrates in *in vitro* kinase reactions, we saw that CDK targeted specifically only the second serine in each peptide, although much stronger for S222 than for S134, consistent with these residues matching CDK consensus motifs (Fig 1C). In contrast, DDK showed only little activity towards the non-phosphorylated peptides, but was strongly stimulated when the second residue in the (S/T)(S/T) motif was in a phosphorylated state (Fig 1C). DDK may thus be stimulated by priming phosphorylation in order to efficiently phosphorylate Mms4 on (S/T)(S/T) sites. However, using the full-length protein as a phosphorylation substrate, we did not obtain evidence for a stimulatory effect on DDK by prior CDK phosphorylation (Fig 1B and Appendix Fig S1C), perhaps because over the whole 15 (S/T)(S/T) motifs CDK phosphorylation plays a minor role. We also did not reveal any priming activity of either CDK or DDK for Mms4 phosphorylation by Cdc5 (Fig 1B and Appendix Fig S1D). Overall, the data in Fig 1 thus identify Mus81-Mms4 as an interaction partner and potential substrate of DDK.

### Mus81-Mms4 is phosphorylated by a mitotic Cdc5-DDK complex

DDK is present and active throughout S phase and mitosis until anaphase when the Dbf4 subunit is degraded by APC/C<sup>Cdc20</sup> (Cheng *et al*, 1999; Weinreich & Stillman, 1999; Ferreira *et al*, 2000). We therefore tested at which cell cycle stage DDK would associate with Mus81-Mms4 using cells synchronously progressing through the cell cycle. Figure 2A shows that DDK did not associate with Mus81-Mms4 in S phase, but only once cells had reached mitosis. Strikingly, DDK binding therefore coincided with binding of Cdc5, Slx4 and Dpb11 and most notably the appearance of the hyperphosphorylated form of Mms4<sup>3FLAG</sup> (Fig 2A).

Given this late timing of the association, we tested in co-immunoprecipitation (co-IP) experiments whether DDK binding to Mus81-Mms4 would depend on CDK or Cdc5 activity. Using analog-sensitive mutant yeast strains for CDK [*cdc28-as1* (Bishop *et al*, 2000)] and for Cdc5 [*cdc5-as1* (Snead *et al*, 2007)], we observed that inhibition of these kinases in mitotically arrested cells strongly reduced the hyperphosphorylation shift of Mms4 (see also Matos

*et al*, 2013) and compromised the association with DDK (Fig 2B and C, and Appendix Fig S2A–C). Notably, both conditions also interfered with Cdc5 binding (Fig 2B and C, and Appendix Fig S2A), suggesting that the association of DDK may follow a similar regulation as Cdc5.

Next, we tested whether conversely DDK is involved in Mms4 phosphorylation. To bypass the essential function of DDK in DNA replication, we used the *mcm5<sup>bob1-1</sup>* allele (Hardy *et al*, 1997), which allowed us to test a *cdc7Δ* mutant. Using Western blot and SILAC-based mass spectrometry as a read-out of Mms4<sup>3FLAG</sup> co-IPs from cells arrested in mitosis, we found that Cdc5 association with Mus81-Mms4 was strongly reduced in the *cdc7Δ* mutant strain (Fig 2D and E). Moreover, we observed that Mms4<sup>3FLAG</sup> phosphorylation as indicated by mobility shift was decreased in the absence of DDK, although not to the same extent as upon CDK or Cdc5 inhibition (Fig 2D and Appendix Fig S2C). Additionally, as an alternative way to deregulate DDK, we used the *cdc7-1* temperature-sensitive mutant. Even with WT cells, we observed that elevated temperature (38°C) leads to a slight reduction in Cdc5 binding to Mus81-Mms4. However, in *cdc7-1* mutant cells, incubation at 38°C leads to the complete disappearance of Cdc5 binding to Mus81-Mms4 (Appendix Fig S2D). Therefore, we conclude from these data that DDK and Cdc5 bind to Mus81-Mms4 in an interdependent fashion.

Interestingly, Cdc5 was previously shown to interact with DDK via a non-consensus polo-box binding site within Dbf4 (Miller *et al*, 2009; Chen & Weinreich, 2010). The proposed model based on genetic experiments suggested that DDK binding antagonizes mitotic functions of Cdc5. However, the catalytic activity of Cdc5 was not inhibited in this complex (Miller *et al*, 2009) and we reason that DDK may simply target Cdc5 to a specific set of substrates. Since the Cdc5 binding site was mapped to the N-terminal portion of Dbf4 (Miller *et al*, 2009), we tested whether N-terminal truncations of Dbf4 would affect DDK or Cdc5 association with Mus81-Mms4. While the *dbf4-ΔN66* truncation lacking the first 66 amino acids (including a D-box motif) did not influence DDK or Cdc5 binding to Mms4<sup>3FLAG</sup>, the *dbf4-ΔN109* truncation, which additionally lacks the Cdc5 binding motif (Miller *et al*, 2009), showed strongly decreased DDK and Cdc5 binding to Mus81-Mms4 (Fig 2F). Additionally, also mitotic hyperphosphorylation of Mms4 was diminished when DDK and Cdc5 could not interact with each other (Fig 2F). Overall, these data strongly suggest that Cdc5 and DDK interact with and target Mus81-Mms4 in an interdependent manner. Furthermore, it is currently unclear whether collaboration of DDK and Cdc5 is a widespread phenomenon that may affect other Cdc5 substrates as well, given that mitotic phosphorylation of two candidate Cdc5 substrates, Ulp2 and Scc1 (Alexandru *et al*, 2001), was affected to varying degree by the *cdc7Δ* mutation (Appendix Fig S2E).

Given the known cell cycle regulation of Cdc5 and DDK (Shirayama *et al*, 1998; Cheng *et al*, 1999; Weinreich & Stillman, 1999; Ferreira *et al*, 2000; Mortensen *et al*, 2005), the limiting factor for the temporal regulation of this complex and its restriction to mitosis is expected to be Cdc5 and not DDK, which is present already throughout S phase. Consistently, we observed that forced expression of Cdc5 (using the galactose-inducible GAL promoter) in cells that were arrested in S phase by hydroxyurea (HU) led to the premature occurrence of Mms4

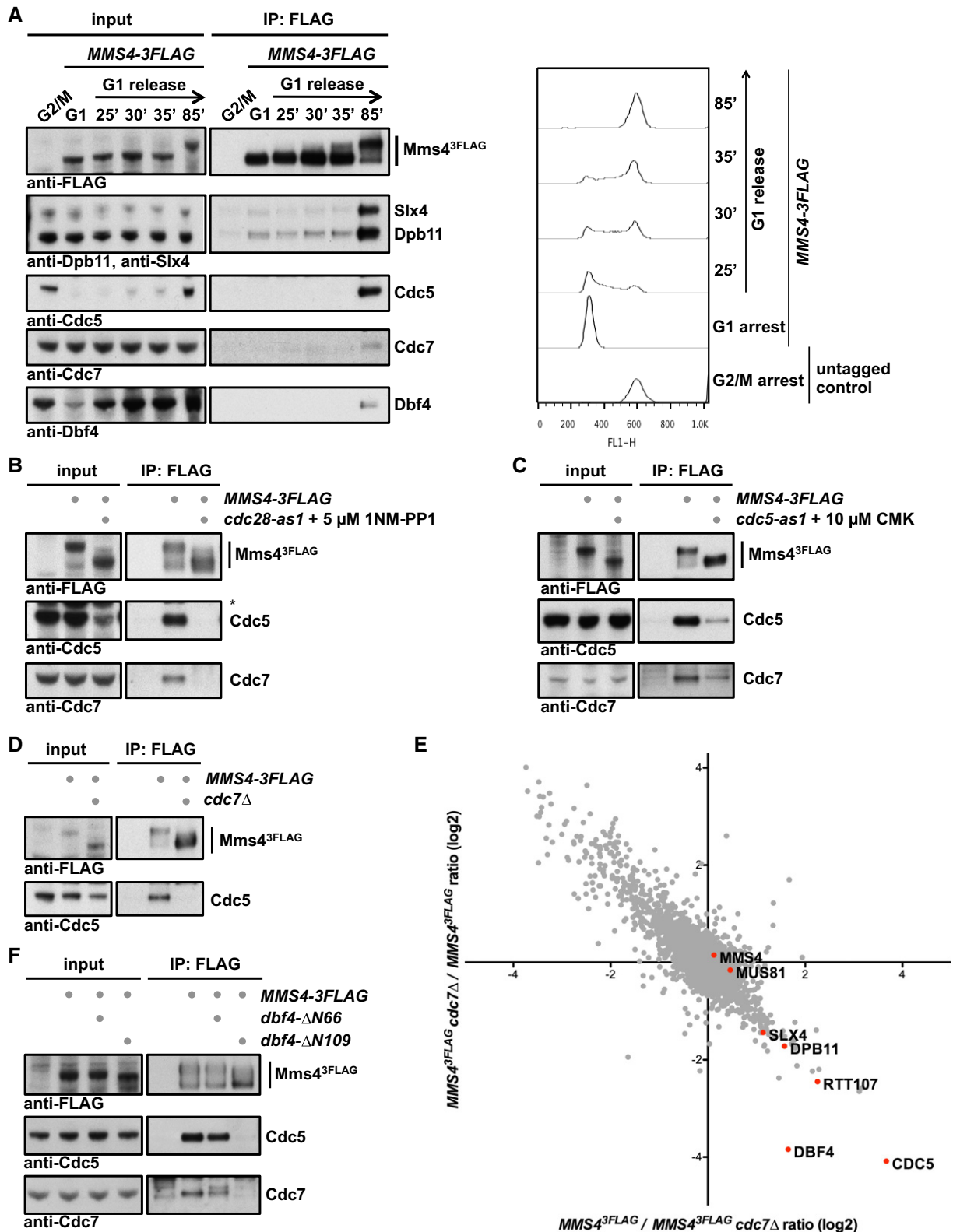


Figure 2.

hyperphosphorylation (Fig EV1A; Matos *et al*, 2013), suggesting that S-phase DDK is in principle competent for Cdc5 binding and joint substrate phosphorylation.

Furthermore, we performed additional experiments that addressed the regulation of Mus81-Mms4 by the DNA damage response. In M-phase-arrested cells, association of DDK and

**Figure 2. DDK and Cdc5 target Mus81-Mms4 in an interdependent manner.**

- A DDK stably associates with Mus81-Mms4 in mitosis, but not in S phase or G1. Mms4<sup>3FLAG</sup> pull down experiment (left panel, as in Fig 1A) from cells arrested in G1 (with alpha-factor) or in cells progressing synchronously through S phase until mitosis (arrest with nocodazole) reveals that DDK binds specifically in mitosis concomitant with the raise in Cdc5 levels and Cdc5 binding to Mus81-Mms4. A nocodazole-arrested untagged strain was used as a control. Right panel shows measurements of DNA content by FACS from the respective samples.
- B CDK activity is required for DDK and Cdc5 association with Mus81-Mms4. Mms4<sup>3FLAG</sup> pull down as in (A), but in mitotic WT or *cdc28-as1* mutant cells treated with 5  $\mu$ M 1NM-PP1 for 1 h. Additional Western blots of this experiment are shown in Appendix Fig S5B, including as a control the identical anti-FLAG Western blot.
- C Cdc5 activity is required for DDK association with Mus81-Mms4. Mms4<sup>3FLAG</sup> pull down as in (A), but with mitotically arrested WT or *cdc5-as1* mutant cells treated with 10  $\mu$ M CMK for 1 h.
- D, E DDK is required for Cdc5 binding to Mus81-Mms4 in mitosis and the mitotic Mms4 phospho-shift. (D) Mms4<sup>3FLAG</sup> pull down using mitotically arrested cells as in (A), but using a *bob1-1* background (all samples), where the DDK subunit Cdc7 could be deleted. (E) SILAC-based quantification of Mms4<sup>3FLAG</sup> pull downs in mitotically arrested *bob1-1* vs. *bob1-1 cdc7 $\Delta$*  cells. Plotted are the H/L ratios of two independent experiments including label switch.
- F The Cdc5 binding region on Dbf4 is required for interaction of DDK and Cdc5 with Mus81-Mms4 and for efficient Mms4 phosphorylation. Mms4<sup>3FLAG</sup> pull down as in (A), but using mitotically arrested cells expressing N-terminal truncation mutants of Dbf4 lacking aa2–66 (including a D-box motif) or 2–109 [additionally including the Cdc5 binding site (Miller *et al.*, 2009)].

Cdc5 with Mus81-Mms4 was reduced after induction of DNA damage with phleomycin (Appendix Fig S2F), but this treatment was not sufficient to induce a significant reduction in the Mms4 phosphorylation shift. Interestingly, when we forced Cdc5 expression in S-phase cells and compared normal S-phase cells to cells treated with hydroxyurea (HU), we observed that the Mms4 phosphorylation shift was less pronounced in the presence of hydroxyurea (HU) (Fig EV1B). These data are therefore consistent with the current view that DNA damage, specifically the DNA damage checkpoint, negatively influences Mus81 resolution activity (Szakal & Branzei, 2013; Gritenaite *et al.*, 2014). Since DDK is known to be targeted and inhibited by the DNA damage checkpoint (Weinreich & Stillman, 1999; Lopez-Mosqueda *et al.*, 2010; Zegerman & Diffley, 2010), it could become particularly critical to regulate Mms4 phosphorylation after DNA damage.

Even though DDK and Cdc5 seem to target Mus81-Mms4 in unison, we tested whether it was possible to resolve differences on the level of individual phosphorylation sites. Therefore, we analysed Mms4 phosphorylation sites in M-phase cells after Cdc5 inhibition (Fig 3A and C) or *CDC7* deletion (Fig 3B and D) by SILAC-based mass spectrometry. We also applied two different experimental set-ups that used either endogenously expressed Mus81-Mms4 (Fig 3A and B) or overexpressed Mus81-Mms4 (Fig 3C and D), as the latter set-up allowed much better coverage of Mms4 phosphopeptides in higher order phosphorylation states (peptides harbouring > 1 phosphorylated site). Cdc5 inhibition or lack of DDK led to overlapping, but distinct changes in Mms4 phosphorylation sites, suggesting that each kinase phosphorylates specific sites on Mms4. After Cdc5 inhibition, phosphorylation of many sites was reduced and among those were sites that match to a putative Cdc5 consensus [(D/E/N)X(S/T), blue, Fig 3A and C; Mok *et al.*, 2010]. Overall, *CDC7* affected Mms4 phosphorylation less than Cdc5 inhibition, but nonetheless, we found widespread changes in the phosphorylation of (S/T)(S/T) motifs (Fig 3B and D). (S/T)(S/T) motifs were found less abundantly in the doubly phosphorylated state (Fig 3D, red), while conversely these motifs were found more abundantly in the state where only the second (S/T) was singly phosphorylated (Fig 3B and D, yellow), as expected for a substrate–product relation. These data are thus consistent with phosphorylation of the second (S/T) priming for phosphorylation at the preceding (S/T) (Appendix Table S1 and Appendix Fig S3).

### DDK phosphorylation is required for activation of Mus81-Mms4 during mitosis

Phosphorylation of Mms4 by CDK and Cdc5 has previously been shown to be required for the upregulation of Mus81-Mms4 activity during mitosis (Matos *et al.*, 2011, 2013; Gallo-Fernández *et al.*, 2012; Szakal & Branzei, 2013). Based on our finding that hyperphosphorylation of Mms4 was impaired in the absence of DDK (Fig 2D and Appendix Fig S2C), we predicted that also Mus81-Mms4 activity would be influenced. Therefore, we tested the activity of endogenous Mus81<sup>9myc</sup>-Mms4<sup>3FLAG</sup> immunopurified from G2/M arrested cells (approx. 5 fmol) on a nicked Holliday junction (nHJ) substrate (500 fmol) using an assay related to those in (Matos *et al.*, 2011, 2013; Gritenaite *et al.*, 2014). Notably, the activity of the endogenous purified Mus81-Mms4 from G2/M cells exceeded the activity of recombinant Mus81-Mms4 (subjected to a dephosphorylation step during the purification), indicating that it is the mitotically activated form (Appendix Fig S4A). Moreover, the activity of endogenous purified Mus81-Mms4 was not influenced by 350 mM NaCl salt washes. This indicates that the presence of accessory, salt-labile factors such as Rtt107 or Cdc5 in the reaction is unlikely to contribute to Mus81 activity (Appendix Fig S4B and C).

Importantly, when we used this assay to test immunopurified Mus81<sup>9myc</sup>-Mms4<sup>3FLAG</sup> from mitotic cells lacking DDK (*cdc7 $\Delta$*  or *dbf4 $\Delta$* ), we observed a reduced activity compared to Mus81<sup>9myc</sup>-Mms4<sup>3FLAG</sup> from WT cells (Fig 4A and Appendix Fig S4D; also observed with an RF substrate, Appendix Fig S4E). In order to exclude that indirect effects of the *CDC7* deletion may cause the reduction in Mus81 activity, we furthermore created an Mms4 mutant that specifically lacks candidate DDK phosphorylation sites. We chose to mutate (S/T)(S/T) motifs (SS motifs in particular) and created an *mms4-8A* mutant that harboured eight S to A exchanges at the N-terminal (S/T) of the motifs (see Appendix Fig S3A). This mutant appeared less phosphorylated in mitosis as judged by a less pronounced phosphorylation shift (Fig 4B). Furthermore, we observed a reduction in the association of DDK and Cdc5 with the Mus81-Mms4-8A complex in pull-down experiments (Fig 4B), suggesting that phosphorylation of Mms4 also plays a role in tethering these kinases. Notably, Mus81<sup>9myc</sup>-Mms4<sup>3FLAG</sup>-8A from mitotic cells showed a moderate but reproducible reduction in resolution activity on nHJ substrates compared to WT Mus81<sup>9myc</sup>-Mms4<sup>3FLAG</sup> (Fig 4C and Appendix Fig

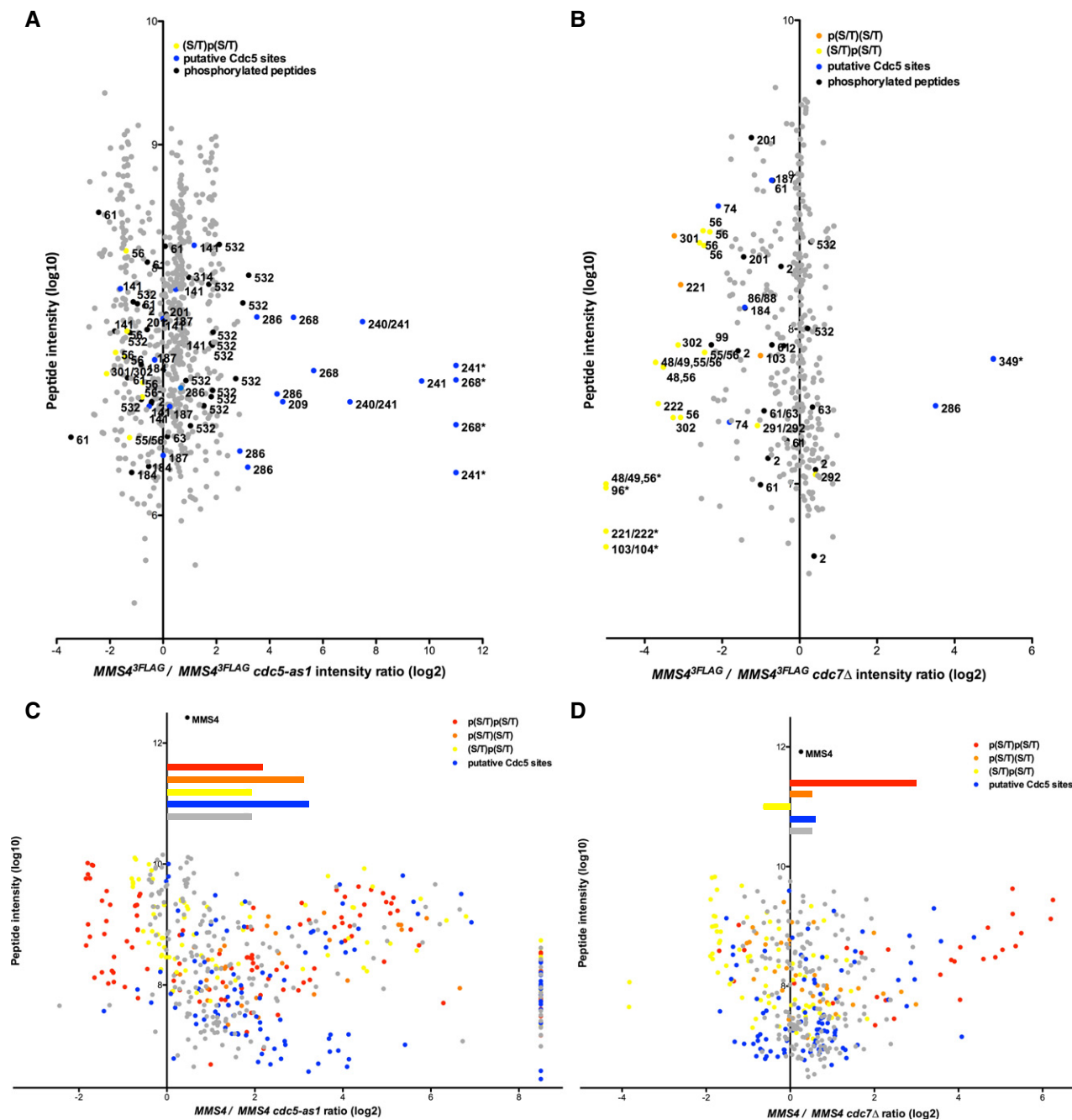


**Figure 3. Analysis of Mms4 phosphorylation sites reveals Cdc5 and DDK target sites, as well as the interdependence between the two.**

Changes of the abundance of phosphorylated Mms4 peptides after Cdc5 inhibition (as in Fig 2C) (A, C) or in the absence of Cdc7 (B, D) in mitotically arrested cells.

A, B Depicted are SILAC-based intensity ratios of individual MS evidences for peptides of endogenously expressed Mms4. Evidences of non-phosphorylated Mms4 peptides are shown in grey; evidences of phosphorylated peptides are shown in black, yellow, orange or blue. Blue colour indicates putative Cdc5 phosphorylation as defined by the (D/E/N)X(S/T) consensus (and additionally S268, which was also very strongly deregulated upon Cdc5 inhibition). Yellow or orange colours mark singly phosphorylated (S/T)(S/T) motifs, with orange marking p(S/T)(S/T) and yellow marking (S/T)p(S/T). Numbers indicate the phosphorylated residue in the depicted peptide. An asterisk marks peptide evidences that contained measured intensity values exclusively in the heavy or light sample. For doubly phosphorylated peptides, the two phospho-sites are separated by a comma. For singly phosphorylated (S/T)(S/T) motifs, peptide ion fragmentation was in some cases unable to unambiguously identify the phosphorylated residue. In these cases, possible phosphorylation sites are indicated as "a/b". Note that doubly phosphorylated (S/T)(S/T) sites were not reproducibly identified under conditions of endogenous Mus81-Mms4 expression.

C, D As in panels (A, B) but using Mus81-Mms4 expressed from a high-copy promoter. Depicted are SILAC-based H/L ratios of individual MS evidences for phosphorylated peptides only. Peptides were sorted into categories according to their phosphorylation status: putative DDK target sites ((S/T)(S/T) motifs) were differentiated into the categories p(S/T)p(S/T) (red), p(S/T)(S/T) (orange) or (S/T)p(S/T) (yellow). Phosphorylated peptides matching the Cdc5 consensus site are coloured in blue. All other phosphorylated peptides are marked in grey. Bars depict the mean of the ratios of the respective category. Overall, Mms4 H/L ratio is shown on top.

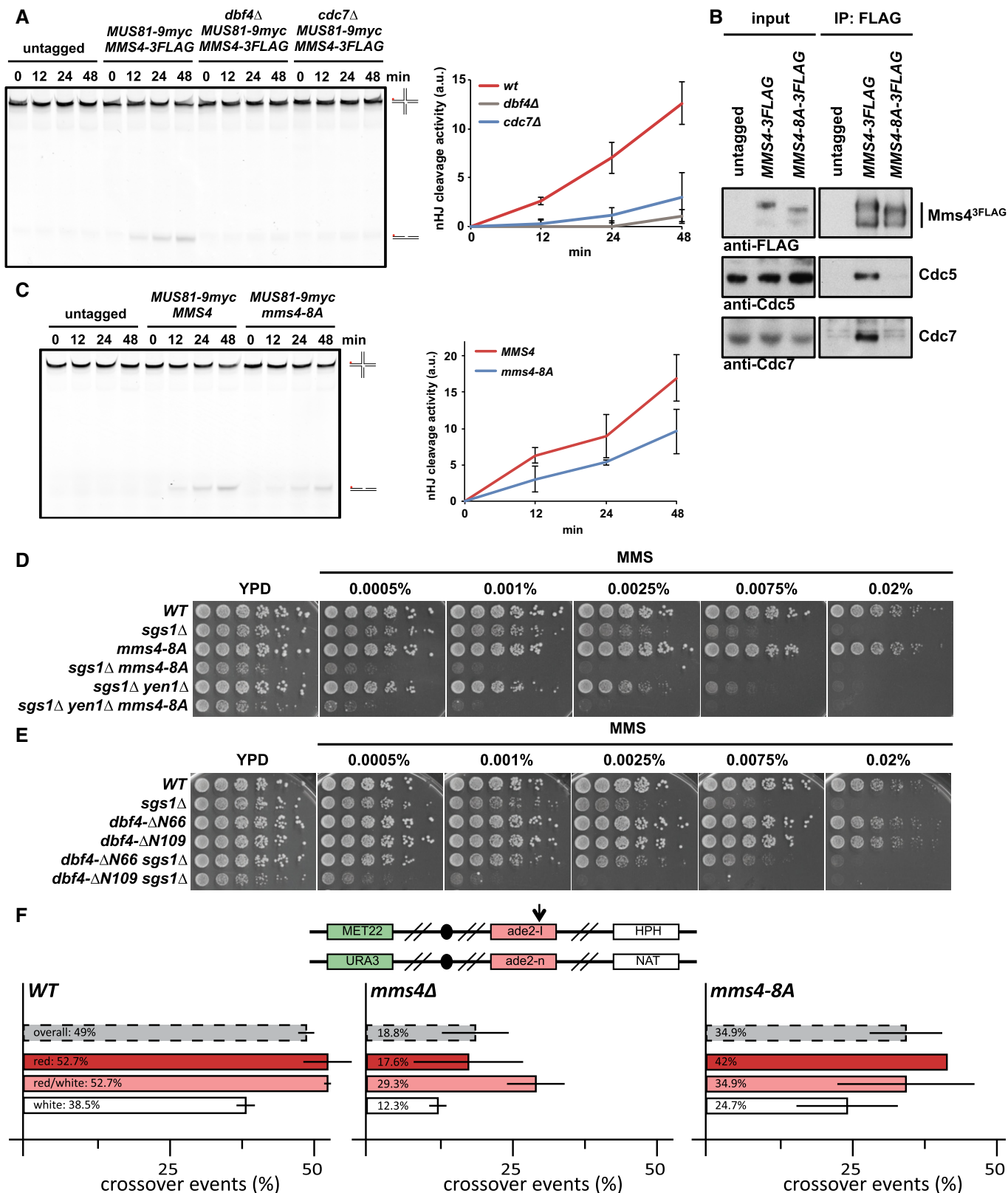


Figure 4.

S4F). These data thus indicate that DDK targets Mus81-Mms4 and that (S/T)(S/T) phosphorylation events are essential for full activation of Mus81 in mitosis.

Additionally, we investigated the relevance of the *mms4-8A* mutation *in vivo*. In comparison with *mus81Δ* or *mms4Δ* mutants, the *mms4-8A* mutant showed a hypomorphic phenotype. For

**Figure 4. DDK phosphorylation controls activation of Mus81-Mms4 resolvase activity in mitosis.**

- A DDK is required for mitotic activation of Mus81-Mms4. Resolution assay using a nicked Holliday junction (nHJ) substrate and Mus81<sup>9myc</sup>-Mms4<sup>3FLAG</sup> purified from mitotically arrested *bob1-1* (DDK-WT<sup>+</sup>), *bob1-1 dbf4Δ* and *bob1-1 cdc7Δ* strains or untagged control cells. Right panel: quantification of cleavage products. See Appendix Fig S4D for Western blots samples of anti-myc IPs. Left panel: representative gel image.
- B A defect in the phosphorylation of Mms4 (S/T)(S/T) sites causes reduced association of Cdc5 and DDK with Mus81-Mms4 and reduced phosphorylation of Mms4. Mms4<sup>3FLAG</sup> pull down as in Fig 1A, but using mitotically arrested WT and *mms4-8A* mutant cells, which harbour 8 serine to alanine exchanges at (S/T)(S/T) motifs (detailed in Appendix Fig S3).
- C Reduced (S/T)(S/T) phosphorylation of Mms4 generates a defect in Mus81-Mms4 activity. Resolution assay as in (A), but comparing mitotic Mus81-Mms4 from untagged, WT and *mms4-8A* strains (see Appendix Fig S4F for Western blot samples of anti-myc IPs).
- D, E The *mms4-8A* mutation and lack of the Cdc5-DDK interaction (*dbf4-ΔN109*) lead to hypersensitivity towards MMS specifically in the *sgs1Δ* background. Shown is the growth of indicated strains in fivefold serial dilution on plates containing MMS at indicated concentrations after 2 days at 30°C.
- F The *mms4-8A* mutant leads to a reduction in crossover formation. Recombination assay between heterologous *ade2* alleles in diploid cells as described in Ho et al (2010). The top panel indicates markers on both copies of chromosome XV that are used to determine genetic outcomes of DSB repair. Arrow indicates the I-SceI cut site. Bottom panel indicates rates of crossover events (%) overall (grey) and in the individual classes (red, red/white, white) that differ in gene conversion tract length. Error bars indicate standard deviation of two independent experiments, each scoring 400–600 colonies per strain.

Data information: (A, C) Depicted are means from three independent experiments, error bars correspond to standard deviation.

example, it did neither significantly increase the MMS hypersensitivity of a *yen1Δ* mutant, nor did it confer synthetic lethality with mutants defective in STR function, such as *sgs1Δ*, even though the *mms4-8A sgs1Δ* double mutant displayed a slow growth phenotype (Figs 4D and EV2A). Importantly, however, we did observe a strongly increased hypersensitivity towards MMS, when we tested an *mms4-8A sgs1Δ* double mutant and compared it to an *sgs1Δ* single mutant (Fig 4D). The *mms4-8A* mutation thus leads to a phenotype that is very similar to other activation-deficient *MMS4* mutants in budding and fission yeast (Gallo-Fernández et al, 2012; Dehé et al, 2013; Matos et al, 2013). Remarkably, the MMS hypersensitivity phenotype of the *mms4-8A* mutant was highly similar to that of the Cdc5 binding-deficient *dbf4-ΔN109* mutant (Figs 4E and EV2B), which also showed reduced survival when combined with *sgs1Δ* (Fig 4E). These data are therefore consistent with DDK functioning to stimulate JM resolution via Mms4 hyperphosphorylation.

It is likely that the *mms4-8A* mutant is only partially deficient in DDK phosphorylation, since Mms4 contains overall 15 (S/T)(S/T) sites and DDK may phosphorylate the protein on non-(S/T)(S/T) sites as well. We therefore note that an *mms4-12A* mutant, harbouring four additional S to A exchanges on (S/T)(S/T) motifs, showed further increased MMS sensitivity in the *mms4-12A sgs1Δ* mutant, when compared to the *mms4-8A sgs1Δ* mutant, even though there were only minor additional effects on either the Mms4 mitotic phosphorylation shift or JM resolution activity (Fig EV2C–E).

In order to directly assess whether DDK phosphorylation was required for Mus81 function during JM resolution, we tested the influence of the *mms4-8A* mutant in a genetic crossover assay (Ho et al, 2010). In this system, a site-specific DSB is induced in diploid cells and repair products can be measured by the arrangement of markers and colony sectoring (Fig 4F, upper panel). In this assay, *mus81Δ* and *mms4Δ* mutants show a reduction in CO products and a proportional increase in NCO products (Fig 4F; Ho et al, 2010), as would be expected from a defect in JM resolution and the accompanying shift of repair pathways towards JM dissolution. The *mms4-8A* mutant shows a similar, albeit weaker defect in the formation of CO products (Fig 4F), suggesting that the defect in Mus81 activation in mitosis results in an overall defect in JM resolution. We therefore conclude that DDK—in conjunction with Cdc5—acts directly on Mms4 and that these phosphorylation events are required for efficient Mus81-dependent JM resolution in mitosis.

**The Dpb11-Mms4 interaction is not required for DDK-Cdc5-dependent activation of Mus81-Mms4**

It is noteworthy that the association of DDK and Cdc5 with Mus81-Mms4 coincides with the formation of the Mus81-Mms4 complex with scaffold proteins such as Slx4, Dpb11 and Rtt107, which come together in mitosis (Fig 2A). Therefore, we asked whether the scaffold proteins Dpb11, Slx4 or Rtt107 would be required to target DDK and Cdc5 to Mus81-Mms4. In order to investigate the influence of Dpb11, we searched for an *MMS4* mutant that was deficient in the interaction with Dpb11. When we used a two-hybrid approach to map the Dpb11 interaction site on Mms4, we found that Mms4 constructs comprising aa 1–212 or 101–230 interacted with Dpb11, while constructs comprising aa 1–195 or 176–230 showed no or reduced interaction (Appendix Fig S5A). This suggested that the Dpb11 binding site may be located between aa 101–212 of Mms4. Consistently, we observed that the Mms4-S201A mutation abolished binding to Dpb11 in yeast two-hybrid and co-IP (Fig 5A and B), while the Mms4-S184A mutation reduced it (Fig 5A). Serine 201 and 184 are therefore likely candidates for phospho-sites bound and read by Dpb11. Serine 201 matches the full CDK consensus motif (S/T)PxK, while serine 184 matches the minimal CDK consensus motif (S/T)P. Indeed, we find that CDK inhibition reduced the Dpb11 interaction with Mus81-Mms4 (Appendix Fig S5B) consistent with a requirement of CDK phosphorylation for a robust interaction between Dpb11 and Mms4.

When we investigated the phenotype of the *mms4-SS184,201AA* mutant, we found that it showed enhanced hypersensitivity to MMS specifically in the *sgs1Δ* mutant background, consistent with a role of Dpb11 in JM resolution after MMS damage (Fig 5C). We also noted that the phenotype of this *MMS4* variant differed from that induced by Dpb11 binding-deficient version of Slx4 [*slx4-S486A* (Gritenaite et al, 2014; Ohouo et al, 2012)]. This could suggest that these mutants are able to separate different Dpb11 functions such as a mitotic function in conjunction with Mus81-Mms4 and an S-phase function, which Slx4 and Dpb11 might have independently of Mus81-Mms4 (Ohouo et al, 2012; Gritenaite et al, 2014; Cussiol et al, 2015; Princz et al, 2015). However, it also needs to be considered that Slx4 and Mus81-Mms4 may be connected by more than one scaffold protein (see below).

Importantly, however, we did not observe a defect in the association of DDK or Cdc5 with Mus81-Mms4, when we performed

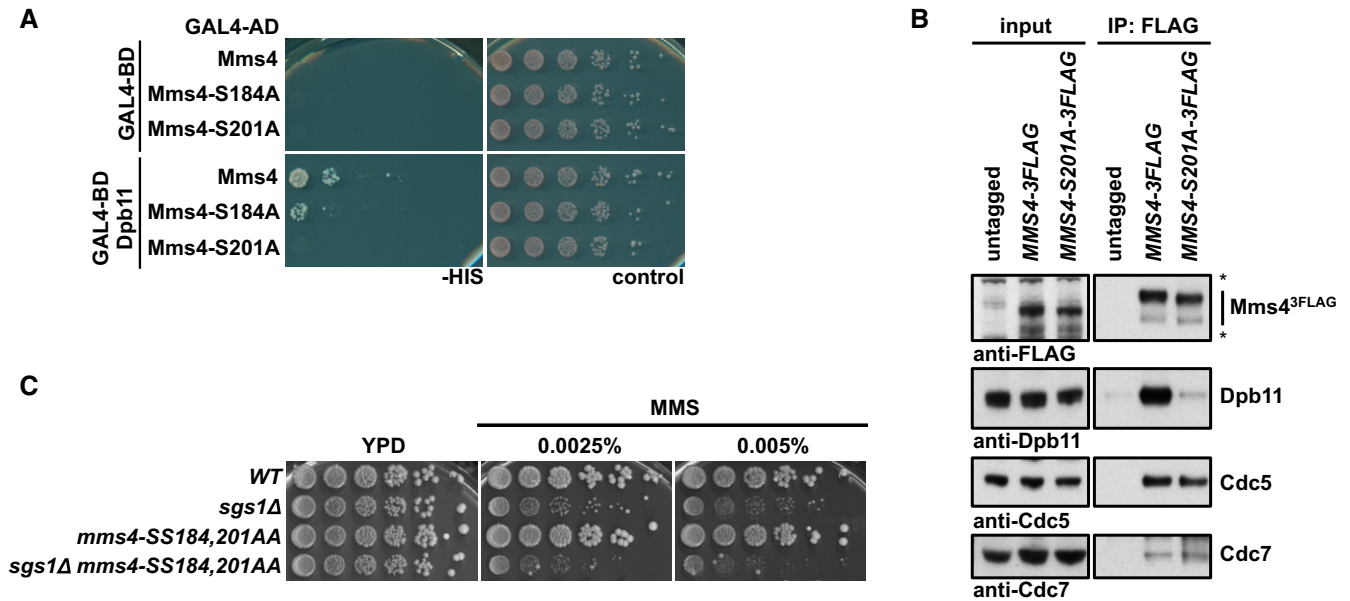


**Figure 5. The interaction between Mms4 and Dpb11 is dispensable for binding of Cdc5 and DDK and mitotic Mus81-Mms4 activation.**

A, B Serine 201 of Mms4 is required for Dpb11 binding, but not for interaction with DDK and Cdc5. (A) Two-hybrid interaction analysis using Gal4-BD-Dpb11 with Gal4-AD-Mms4, Gal4-AD-Mms4-S184A and Gal4-AD-Mms4-S201A constructs. (B) Mms4<sup>3FLAG</sup> pull downs from mitotically arrested cells as in Fig 1A, but using WT or S201A variants of Mms4<sup>3FLAG</sup>. Asterisks mark cross-reactive bands.

C The Dpb11 binding-deficient allele *mms4-SS184,201AA* leads to a MMS hypersensitivity specifically in the *sgs1Δ* background. Spotting assay as in Fig 4D.

Mms4-S201A<sup>3FLAG</sup> pull downs and compared them to a WT Mms4<sup>3FLAG</sup> pull down (Fig 5B). Furthermore, we only observed a very minor defect in the *in vitro* resolution of nHJ substrates, when we purified Mus81-Mms4 from mitotically arrested *mms4-S201A* cells (Appendix Fig S5C). We therefore reason that Dpb11 is most likely not involved in promoting Mms4 phosphorylation or DDK-Cdc5-dependent activation of Mus81-Mms4.

#### The Rtt107 scaffold recruits DDK and Cdc5 to Mus81-Mms4

Having excluded a role of Dpb11 in the recruitment of DDK and Cdc5, we next tested a possible involvement of the Rtt107 scaffold protein. Indeed, when we used an *rtt107Δ* mutant in IP and SILAC-based IP-MS experiments, we observed that DDK and Cdc5 binding to Mus81-Mms4 was strongly reduced (Fig 6A and Appendix Fig S6A). Interestingly, Rtt107 bound to DDK and Cdc5 even under conditions where Rtt107 binding to Mus81-Mms4 was abolished (*mus81Δ*, Appendix Fig S6B). This suggests that Rtt107 may form a subcomplex with DDK and Cdc5. Consistently, we found that Rtt107 bound to Cdc7 in a two-hybrid assay (Fig 6B). These data therefore suggest that Rtt107 mediates binding of DDK and Cdc5 to the Mus81-Mms4 complex, most likely via a Cdc7 interaction site on Rtt107.

During our co-IP studies, we furthermore found that the location of Rtt107 in the mitotic Mus81-Mms4 complex was different than expected. Given that Slx4 was required to bridge between Rtt107 and Dpb11 (Ohouo *et al*, 2010) and that Mms4 and Dpb11 seemingly interact directly (Gritenaite *et al*, 2014 and Fig 5A and B), we initially expected that Slx4 and Dpb11 would be required to mediate the interaction between Rtt107 and Mus81-Mms4. Surprisingly, we found that an *slx4Δ* mutant did not influence DDK or Cdc5 binding

to Mus81-Mms4 and thereby differed from *rtt107Δ* (Fig 6A). Therefore, we tested if Rtt107 could bind to Mus81-Mms4 independently of Slx4 or Dpb11. Indeed, we found that the Mus81-Mms4 interaction to Rtt107 was not influenced by the *slx4Δ* mutant (Fig 6C) or the Dpb11 binding-deficient *mms4-S201A* allele (Fig 6D), indicating that Rtt107 binding to the Mus81-Mms4 complex occurs independently of the other scaffold proteins. In contrast, our data also show that its binding is strongly dependent on kinases and Mms4 phosphorylation, since Rtt107 binding was strongly reduced in the absence of DDK (Fig 2E), after Cdc5 inhibition (Appendix Fig S2A) or in the *mms4-8A* phosphorylation site mutant (Fig EV3).

Therefore, these data provide novel insight into the role of Rtt107 in Mus81-Mms4 regulation. First, it shows that Rtt107 mediates the association of DDK and Cdc5 kinases with Mus81-Mms4. Second, it also suggests that Rtt107 may bind directly to Mus81-Mms4 and that this binding is dependent on Mms4 phosphorylation and the cell cycle kinases DDK and Cdc5, although an alternative model whereby Rtt107 indirectly promotes DDK and Cdc5 to tightly associate with Mus81-Mms4 cannot be ruled out entirely. The fact that Rtt107 promotes the interaction of Mus81-Mms4 with the kinases, yet in turn requires the kinases and Mms4 phosphorylation for interaction, suggests that Rtt107 may be acting after initial Mms4 phosphorylation has occurred and at this late stage tethers the kinases, thus promoting phosphorylation of otherwise inefficiently phosphorylated sites.

#### Rtt107 stimulates Mms4 hyperphosphorylation in order to enhance Mus81-Mms4 activity in mitosis

Given Rtt107's involvement in tethering DDK and Cdc5 to the Mus81-Mms4 complex, we asked whether Rtt107 would mediate

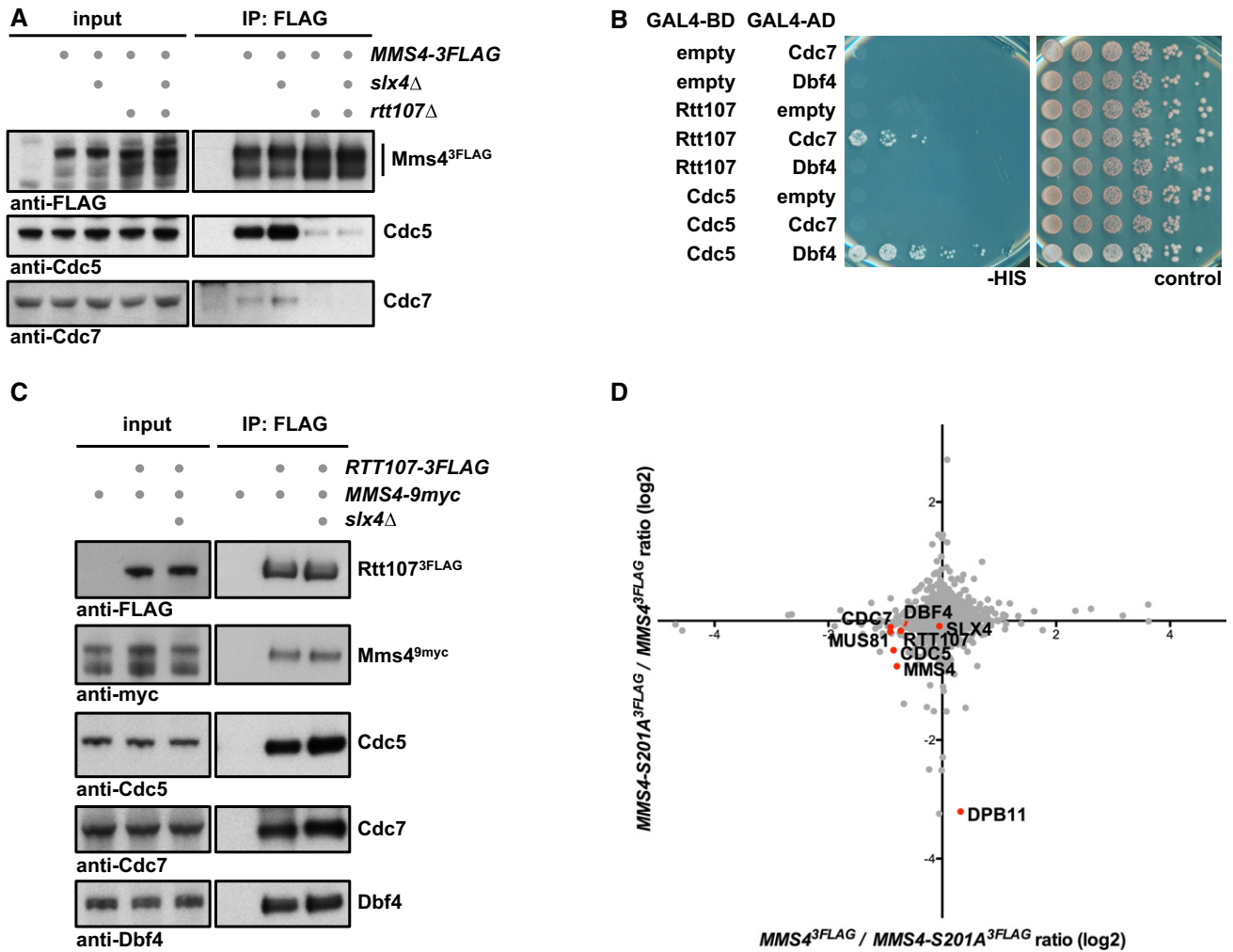


**Figure 6. The Rtt107 scaffold tethers DDK and Cdc5 to Mus81-Mms4 independently of Slx4 and Dpb11.**

- A Rtt107, but not Slx4, is required for DDK and Cdc5 interaction with Mus81-Mms4. *Mms4<sup>3FLAG</sup>* pull downs from mitotically arrested cells as in Fig 1A, but specifically comparing interactions of Mus81-Mms4 in WT, *slx4Δ*, *rtt107Δ* and *slx4Δ rtt107Δ* mutant backgrounds.
- B Rtt107 interacts with Cdc7. Two-hybrid interaction was tested using Gal4-BD-Rtt107 constructs and Gal4-AD-Cdc7 or Gal4-AD-Dbf4 constructs. Interaction between Gal4-BD-Cdc5 and Gal4-AD-Dbf4 serves as positive control.
- C Rtt107 interacts with Mus81-Mms4, DDK and Cdc5 independently of Slx4. Rtt107<sup>3FLAG</sup> co-IPs from untagged control, WT or *slx4Δ* cells arrested in mitosis were probed for indicated proteins.
- D Rtt107 interacts with Mus81-Mms4 independently of the Mms4-Dpb11 interaction. SILAC-based *Mms4<sup>3FLAG</sup>* pull down in WT and *mms4-S201A* cells reveals changes in the Dpb11 association, but not in Rtt107, Slx4, Cdc5 or DDK binding. Plotted are the H/L ratios of two experiments including label switch.

mitotic hyperphosphorylation of Mms4 and concomitant activation of the Mus81 nuclease. We observed only a minor effect on the mitotic phospho-shift of Mms4 when using *rtt107Δ* mutants (Fig 6A and Appendix Fig S2C). However, as it is still unclear which phosphorylation sites contribute to the Mms4 phospho-shift, we investigated the effect of *rtt107Δ* on individual phosphorylation sites in our mass spectrometry data. Appendix Fig S7A and B shows SILAC-based comparisons of Mms4 phosphorylation sites in WT and *rtt107Δ* cells, expressing Mus81-Mms4 from endogenous (Appendix Fig S7A) or high-copy promoters (Appendix Fig S7B). The overexpression set-up allowed us to quantify phosphorylation at (S/T)(S/T) motifs, and we found that double phosphorylation of several of these sites was reduced (Appendix Fig S7B), although the change was much smaller compared to cells lacking DDK. On the

other hand, while we could not detect higher order phosphorylated Mms4 peptides using endogenous Mus81-Mms4, we could detect an effect of Rtt107 on several other sites (T209, S241 and S268, and to a lesser extent S286; Appendix Fig S7A), which were also deregulated after Cdc5 inhibition (Fig 3A and C). These data are thus consistent with Rtt107 promoting efficient DDK and Cdc5 phosphorylation of Mms4.

Therefore, we tested whether Rtt107 would affect the mitotic activation of Mus81-Mms4. We immunopurified Mus81<sup>9myc</sup>-Mms4<sup>3FLAG</sup> from WT and *rtt107Δ* cells that were arrested in mitosis and found that Mus81-Mms4 activity on a nHJ substrate was reduced in the *rtt107Δ* background (Fig 7A and Appendix Fig S7C). Furthermore, in the background of deficient DDK (*cdc7Δ bob1-1*), additional mutation of *rtt107Δ* did not lead to a further defect in

Mus81-mediated cleavage (Appendix Fig S7D). Therefore, we conclude that Rtt107 is required for full mitotic activation of Mus81-Mms4 and that it works at least in part through cell cycle kinases such as DDK.

In order to test whether such a defect in Mus81-Mms4 activation would translate into a shifted balance of JM removal pathways, we measured rates of crossover and non-crossover formation in the absence of Rtt107. We observed a reduction in crossover rates in the *rtt107Δ* mutant indicating a shift in the balance of JM removal pathways (Fig 7B). The decrease was mostly visible in one class of recombinants (Fig 7B, “red”) and is smaller compared to the phenotype of a *mus81Δ* or a *mms4-8A* mutant (Ho et al, 2010; Fig 4F), consistent with a stimulatory but non-essential role of the Rtt107

scaffold in Mus81-Mms4 function. These data thus provide the first mechanistic insight of how the interaction of the mitotic Mus81-Mms4 complex with the scaffold proteins influences Mus81 function, as Rtt107 facilitates DDK and Cdc5 tethering, full mitotic phosphorylation of Mms4 and activation of Mus81-Mms4.

## Discussion

Activation of Mus81-Mms4 during mitosis is critical for the response to DNA damage, in particular to process repair intermediates that may arise from DSBs and stalled replication forks (Matos et al, 2011, 2013; Gallo-Fernández et al, 2012; Saugar et al, 2013; Szakal

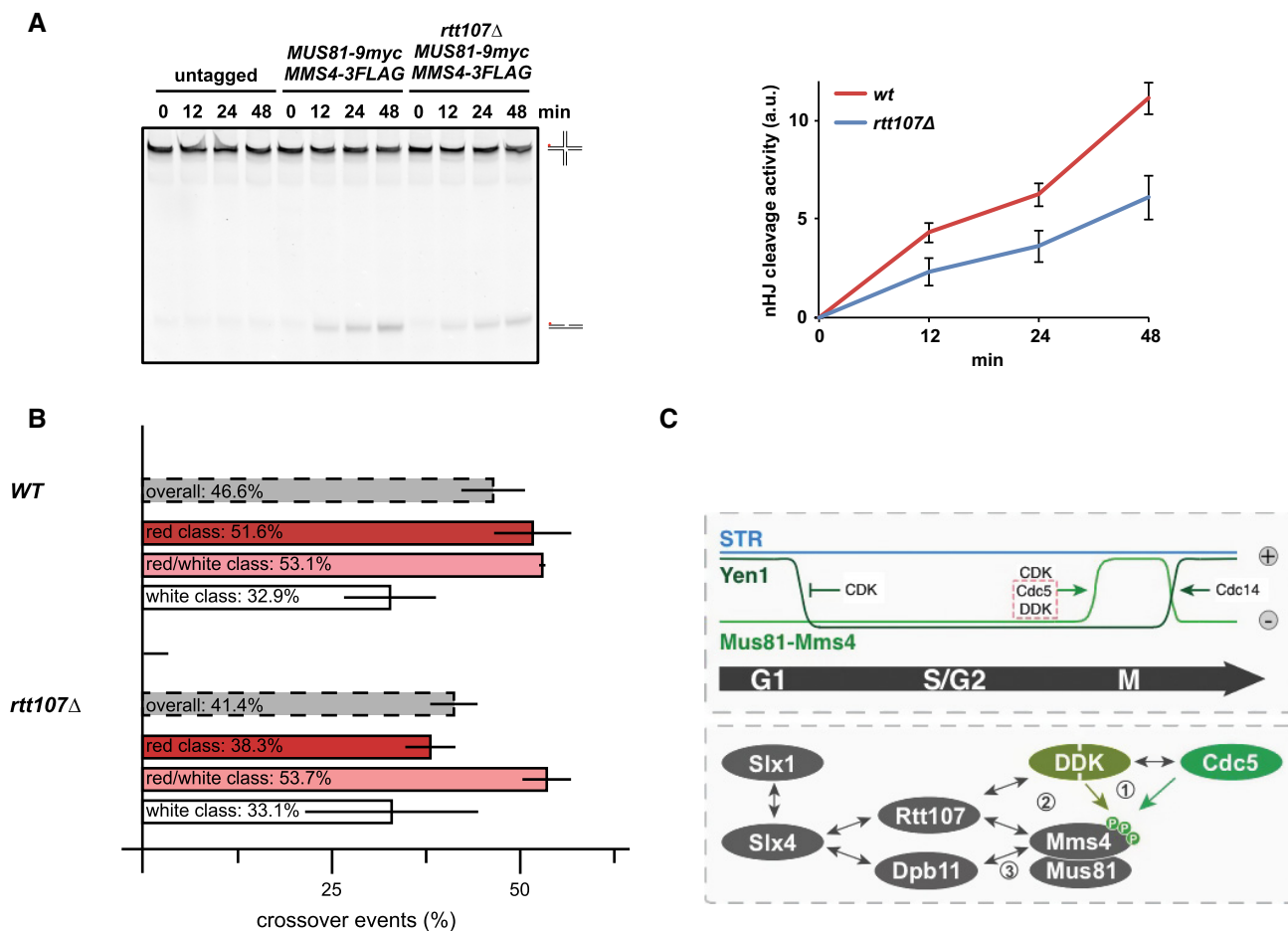


**Figure 7. Rtt107 is required for efficient Mus81-Mms4 activation in mitosis.**

**A** Mus81-Mms4 purified from mitotic *rtt107Δ* cells is less active compared to Mus81-Mms4 from WT cells. *In vitro* resolution activity of Mus81<sup>9myc</sup>-Mms4<sup>3FLAG</sup> purified from WT or *rtt107Δ* cells is tested on a nHJ substrate (see Appendix Fig S7C for control Western blot). Right panel: quantification of cleavage products from three independent experiments (mean ± SD). Left panel: representative gel picture.

**B** The *rtt107Δ* mutant leads to a reduction in crossover formation. Recombination assay as in Fig 4F. Note that the *rtt107Δ* mutant particularly affects crossover formation in the red class (long conversion tracts), while no significant defect could be observed in the red/white and white class (mean ± SD).

**C** Hypothetical model of Mus81-based JM resolution. Upper panel: cell cycle regulation of JM removal pathways, indicating Mus81 activation in mitosis. Lower panel: physical interactions of Mus81-Mms4 and its regulatory complex in mitotic cells. Grey arrows indicate physical interactions; green arrows specifically indicate kinase-substrate interactions. Genetic data indicate a hierarchy of molecular events leading to Mus81 activation. (1) DDK, Cdc5 and CDK (not shown) phosphorylate Mms4. (2) Rtt107 binds to DDK and Cdc5 and—in a phosphorylation-dependent manner—associates with Mus81-Mms4. This interaction is either direct or could potentially depend on bridging effects by DDK and Cdc5. Rtt107 promotes the stable interaction of DDK and Cdc5 with Mus81-Mms4 and thus full phosphorylation of Mms4 and Mus81 activation. (3) Upon Mms4 phosphorylation, two scaffold proteins, Rtt107 and Dpb11, bind independently to Mus81-Mms4. Both proteins can also bind to Slx4 enabling two alternative connections of Slx4 with Mus81-Mms4.

& Branzei, 2013). Previously, this regulation was shown to critically depend on phosphorylation by the cell cycle kinases CDK and Cdc5 (Matos *et al*, 2011, 2013; Gallo-Fernández *et al*, 2012; Saugar *et al*, 2013; Szakal & Branzei, 2013), but also involve the formation of a multi-protein complex comprising several scaffold proteins (Gritenaite *et al*, 2014). Here, we not only identify a new cell cycle kinase to be crucial for this regulation—DDK—but moreover show that the two regulatory pathways—cell cycle kinase phosphorylation and scaffold complex formation—are connected by Rtt107 (see Fig 7C for a hypothetical model). Rtt107 association depends on active cell cycle kinases and Mms4 phosphorylation, but in turn Rtt107 is required for stable DDK and Cdc5 association with the Mus81-Mms4 complex, as well as full phosphorylation of Mms4 and mitotic activation of Mus81. This study thus extends our mechanistic understanding of the regulatory framework that controls cell cycle-regulated JM resolution.

Interestingly, our work shows that for its function as a regulator of Mus81-Mms4 DDK must act interdependently and as a complex with Cdc5. DDK and Cdc5 have been shown to interact physically (Miller *et al*, 2009; Chen & Weinreich, 2010), but until now DDK was viewed to antagonize mitotic functions of Cdc5 (Miller *et al*, 2009). In contrast, in meiosis I DDK and Cdc5 are known to cooperate in order to promote chromosome segregation and jointly phosphorylate the monopolin and cohesin subunits Lrs4 and Rec8, respectively, as well as the meiotic regulator Spo13 (Matos *et al*, 2008). We now provide the first example for a joint DDK and Cdc5 substrate in the mitotic cell cycle, suggesting that cooperation between DDK and Cdc5 could be a more widespread phenomenon than previously anticipated. The apparent antagonism between DDK and Cdc5 in the regulation of mitotic exit (Miller *et al*, 2009), a canonical Cdc5 function, could be explained if DDK targeted Cdc5 to a specialized subset of substrates rather than to substrates involved in mitotic exit. It is also interesting to note that we could detect significant DDK binding to Mus81-Mms4 only after cells finished S phase (Fig 2A). Therefore, the role of DDK in Mms4 phosphorylation is clearly post-replicative and further challenges a simplified view of DDK as an S-phase kinase (Matos *et al*, 2008). It will therefore be interesting to see whether additional DDK substrates during mitosis can be identified and whether DDK collaborates with Cdc5 for their phosphorylation as well.

Mus81-Mms4 has previously been shown to be cell cycle-regulated and Mms4 to be a critical CDK and Cdc5 phosphorylation target (Matos *et al*, 2011; Gallo-Fernández *et al*, 2012). We add DDK to this already complex regulation. Our data clearly show that phosphorylation of (S/T)(S/T) motifs is critical for Mus81-Mms4 function. The hypomorphic phenotype of the *mms4-8A* mutant (Fig 4C, D and F) is likely due to additional DDK phosphorylation sites either on Mms4 or perhaps even on Mus81. Importantly, DDK does not appear to establish the timing of Mms4 phosphorylation in mitosis, as Cdc5 still seems to be the limiting factor for this temporal control in undisturbed cell cycles (Fig EV1B). However, the fact that activation of Mus81-Mms4 depends on the activity of several kinases makes it a coincidence detector that integrates the activity of several cell cycle regulators. Therefore, it can be envisioned that there are specific cellular conditions under which DDK activity becomes limiting for Mus81-Mms4 activation. Notably, DNA damage checkpoint kinases are known to phosphorylate DDK and counteract its function during S phase (Weinreich & Stillman, 1999; Lopez-Mosqueda *et al*, 2010; Zegerman & Diffley, 2010). Therefore,

it can be speculated that the checkpoint acts as a negative regulator of Mus81-Mms4 activation via inhibition of DDK. Such regulation could therefore explain how the presence of DNA damage restricts Mus81 activity towards replication intermediates (Matos *et al*, 2011, 2013; Saugar *et al*, 2013; Szakal & Branzei, 2013; Gritenaite *et al*, 2014), suggesting that cell cycle and checkpoint pathways converge in the regulation of Mus81.

A second layer of Mus81 regulation relies on the formation of a multi-protein complex, which assembles specifically in mitosis and contains Mus81-Mms4, DDK, Cdc5 and Slx4 as well as the scaffold proteins Dpb11 and Rtt107 (Gritenaite *et al*, 2014). We are only beginning to understand the mechanism whereby this scaffold complex influences Mus81 function. Here, we show that Rtt107, but not Dpb11 or Slx4, promotes the stable association of DDK and Cdc5 with Mus81-Mms4 (Fig 6), suggesting that one function of the multi-protein complex is to promote efficient Mus81-Mms4 phosphorylation. Conversely, our new data as well as our previous work (Gritenaite *et al*, 2014) show that phosphorylation by cell cycle kinases also regulates the formation of the multi-protein complex. In particular, Rtt107 association with Mus81-Mms4 depends strongly on DDK and Cdc5 (Fig 2E and Appendix Fig S2A). A direct interaction of Rtt107 with Mus81-Mms4 seems the most plausible interpretation of our data, although we currently cannot exclude that Rtt107 may facilitate the interaction of DDK and Cdc5 with Mus81-Mms4 without a direct interaction. A possible phosphorylation dependence of Rtt107 binding to the complex could thus originate from Mms4 phosphorylation generating a binding site for Rtt107 [e.g. for Rtt107 BRCT domains (Li *et al*, 2012)].

Importantly, Rtt107 is in turn required for stable binding of DDK and Cdc5 (Fig 6A and Appendix Fig S6A). Via tethering the kinases, Rtt107 regulates the phosphorylation of specific Mms4 sites and is required for full Mus81 activation (Fig 7A and Appendix Fig S7A and B). The interdependence between Rtt107 and Cdc5/DDK phosphorylation therefore suggests that Rtt107 may be part of a signal amplification mechanism, which ensures efficient Mus81-Mms4 phosphorylation and activation. Mechanistically, Rtt107-dependent stimulation of Mms4 phosphorylation thus resembles a kinase priming mechanism. It is entirely possible that other kinase priming mechanisms for either Cdc5 or DDK are at work in the Mms4 phosphorylation cascade, although the *in vitro* kinase assays with full-length proteins did not provide support for such a mechanism (Fig 1B, and Appendix Fig S1C and D). Altogether, it seems plausible to speculate that Rtt107-dependent and Rtt107-independent amplification mechanisms are involved in generating a switch-like activation of Mus81 in mitosis.

Furthermore, Rtt107 can also bind to Slx4 (Ohouo *et al*, 2010). There are thus two BRCT-containing scaffold proteins—Dpb11 (Gritenaite *et al*, 2014) and Rtt107—that could bridge between Mus81-Mms4 and Slx4. Interestingly, our data with different *mms4* mutants suggest that either one of these BRCT scaffold proteins is sufficient to connect Slx4 and Mus81-Mms4 [Figs 6D and EV3; note that the *rtt107Δ* mutant (Appendix Fig S6A) is difficult to interpret in this regard as it also leads to defects in Slx4 phosphorylation and the Slx4-Dpb11 interaction (Ohouo *et al*, 2010)]. This redundancy may thus explain the modest phenotype of the *mms4-S201A* mutant that is deficient in the Mms4-Dpb11 interaction (Fig 5C).

Several aspects of Mus81-Mms4 regulation are conserved throughout eukaryotic evolution. The HJ resolution activity of

Mus81-Eme1 in mammalian cells is cell cycle-regulated (Matos *et al*, 2011; Wyatt *et al*, 2013). Mus81-Eme1 furthermore binds to Slx4 and forms multi-protein complexes (Fekairi *et al*, 2009; Muñoz *et al*, 2009; Svendsen *et al*, 2009; Castor *et al*, 2013; Wyatt *et al*, 2013), albeit these complexes may have a different organization to that in yeast. Therefore, it will be interesting to explore in the future if in human cells DDK is also required for activation of Mus81-Eme1 and if this mechanism may contribute to the anti-tumorigenic activity of DDK inhibitors (Montagnoli *et al*, 2008).

## Materials and Methods

All yeast strains are based on W303 and were constructed using standard methods. Plasmids were constructed using the In-Fusion HD cloning kit (Clontech Laboratories), and mutations were introduced by site-directed mutagenesis. A summary of all yeast strains used in this study can be found in the Appendix Table S2.

Cell cycle synchronization was achieved using alpha-factor (G1), hydroxyurea (S), or nocodazole (mitosis). DNA content was measured by flow cytometry with a BD FACSCalibur system using SYTOX green to stain DNA.

Co-immunoprecipitations of yeast extracts were performed on anti-FLAG agarose resin (Sigma) for 2 h with head-over-tail rotation at 4°C as previously described (Gritenaite *et al*, 2014). After bead washing, proteins were eluted by 3X FLAG-peptide (Sigma), precipitated and separated on 4–12% Bis-Tris gels. For SILAC-based mass spectrometry, cells were labelled with heavy-isotope-labelled lysine (Lys6 or Lys8), and proteins were digested with Lys-C. Mass spectrometry data were analysed using MaxQuant (Cox & Mann, 2008).

Yeast two-hybrid assays, genetic interaction assays, *in vitro* kinase assays and peptide binding assays were performed as described previously (Pfander & Diffley, 2011; Gritenaite *et al*, 2014).

Nuclease assays were done as described (Matos *et al*, 2011, 2013). Briefly, Mus81<sup>9myc</sup> was immunopurified from mitotically arrested cells and mixed with 5'-Cy3-end-labelled nicked Holliday junctions. After incubation at 30°C for the indicated times, the reaction was stopped by proteinase K and SDS for 1 h at 37°C. Products were separated by 10% PAGE, and cleavage efficiency was normalized to the level of immunoprecipitated Mus81<sup>9myc</sup>. Unspecific nHJ cleavage in untagged controls was subtracted in the quantifications.

DSB-induced recombination assays were performed as described (Ho *et al*, 2010). Diploids harbouring I-SceI under the control of the GAL promoter were grown in adenine-rich raffinose medium and arrested in mitosis. Nuclease expression was induced by addition of galactose for 2.5 h. Cells were plated on YPAD and replica plated on YPAD + Hyg + Nat, YPAD + Hyg, YPAD + Nat, SC-Met, SC-Ura and SCR-ADE + Gal media after 3–4 days to classify recombination events.

Detailed experimental procedures are available in the Appendix.

### Data availability

Mass spectrometric datasets are available at EBI PRIDE. DDK and the Rtt107 scaffold promote Mus81-Mms4 resolvase activation during mitosis (2015). PXD005356.

**Expanded View** for this article is available online.

## Acknowledgements

We thank U. Kagerer for technical assistance, D. Gritenaite for early contributions to the project, N. Nagaraj and the proteomics laboratory of the MPIB core facility for proteomics analysis, the MPIB core facility for peptide synthesis and sequencing, J. Diffley and L. Symington for antibodies, plasmid constructs and strains, S. Jentsch, Z. Storchova, C. Biertümpfel and members of the Jentsch and Pfander labs for stimulating discussion and critical reading of the manuscript. Work in the Pfander laboratory is supported by the Max-Planck Society and the German Research Council (DFG). Work in the Matos laboratory is supported by ETH Zürich and the Swiss National Science Foundation (Grants 31003A\_153058 and 155823). Work in the Blanco laboratory is co-financed by Ministerio de Economía y Competitividad and FEDER (RYC-2012-10835 and BFU2013-41554-P). Philipp Wild is supported by an EMBO long-term fellowship (ALTF 475-2015). F. Javier Aguado is supported by a PhD fellowship from the I2C Program of Xunta de Galicia (ED481A-2015/011).

## Author contributions

PW and JM performed *in vitro* resolution assays of Figs 4A and C, 7A, and EV2E, and Appendix Figs S4A, C, E, and S7D and analysed the data. FJA and MGB provided recombinant purified Mus81-Mms4 used in Fig 1B, and Appendix Figs S1C and D, and S4A. All other experiments were performed and analysed by LNP, JB and BP. BP wrote the paper and all authors commented on the manuscript.

## Conflict of interest

The authors declare that they have no conflict of interest.

## References

- Alexandru G, Uhlmann F, Mechtler K, Poupard MA, Nasmyth K (2001) Phosphorylation of the cohesin subunit Scc1 by Polo/Cdc5 kinase regulates sister chromatid separation in yeast. *Cell* 105: 459–472
- Bishop AC, Ubersax JA, Petsch DT, Matheos DP, Gray NS, Blethrow J, Shimizu E, Tsien JZ, Schultz PG, Rose MD, Wood JL, Morgan DO, Shokat KM (2000) A chemical switch for inhibitor-sensitive alleles of any protein kinase. *Nature* 407: 395–401
- Bizard AH, Hickson ID (2014) The dissolution of double Holliday junctions. *Cold Spring Harb Perspect Biol* 6: a016477
- Blanco MG, Matos J, West SC (2014) Dual control of Yen1 nuclease activity and cellular localization by Cdk and Cdc14 prevents genome instability. *Mol Cell* 54: 94–106
- Branzei D, Foiani M (2008) Regulation of DNA repair throughout the cell cycle. *Nat Rev Mol Cell Biol* 9: 297–308
- Castor D, Nair N, Déclais A-C, Lachaud C, Toth R, Macartney TJ, Lilley DMJ, Arthur JSC, Rouse J (2013) Cooperative control of Holliday junction resolution and DNA repair by the SLX1 and MUS81-EME1 nucleases. *Mol Cell* 52: 221–233
- Chen YC, Weinreich M (2010) Dbf4 regulates the Cdc5 polo-like kinase through a distinct non-canonical binding interaction. *J Biol Chem* 285: 41244–41254
- Cheng L, Collyer T, Hardy CF (1999) Cell cycle regulation of DNA replication initiator factor Dbf4p. *Mol Cell Biol* 19: 4270–4278
- Cox J, Mann M (2008) MaxQuant enables high peptide identification rates, individualized p.p.b.-range mass accuracies and proteome-wide protein quantification. *Nat Biotechnol* 26: 1367–1372

- Cussiol JR, Jablonowski CM, Yimit A, Brown GW, Smolka MB (2015) Dampening DNA damage checkpoint signalling via coordinated BRCT domain interactions. *EMBO J* 34: 1704–1717
- Dehé P-M, Coulon S, Scaglione S, Shanahan P, Takedachi A, Wohlschlegel JA, Yates JR, Llorente B, Russell P, Gaillard P-HL (2013) Regulation of Mus81–Eme1 Holliday junction resolvase in response to DNA damage. *Nat Struct Mol Biol* 20: 598–603
- Eissler CL, Mazón G, Powers BL, Savinov SN, Symington LS, Hall MC (2014) The Cdk/Cdc14 module controls activation of the Yen1 Holliday junction resolvase to promote genome stability. *Mol Cell* 54: 80–93
- Fekairi S, Scaglione S, Chahwan C, Taylor ER, Tissier A, Coulon S, Dong M-Q, Ruse C, Yates JR, Russell P, Fuchs RP, McGowan CH, Gaillard P-HL (2009) Human SLX4 is a Holliday junction resolvase subunit that binds multiple DNA repair/recombination endonucleases. *Cell* 138: 78–89
- Ferreira MF, Santocanale C, Drury LS, Diffley JF (2000) Dbf4p, an essential S phase-promoting factor, is targeted for degradation by the anaphase-promoting complex. *Mol Cell Biol* 20: 242–248
- Ferretti LP, Lafranchi L, Sartori AA (2013) Controlling DNA-end resection: a new task for CDKs. *Front Genet* 4: 1–7
- Gallo-Fernández M, Saugar I, Ortiz-Bazán MÁ, Vázquez MV, Tercero JA (2012) Cell cycle-dependent regulation of the nuclease activity of Mus81–Eme1/Mms4. *Nucleic Acids Res* 40: 8325–8335
- Gritenaite D, Princz LN, Szakal B, Bantele SCS, Wendeler L, Schilbach S, Habermann BH, Matos J, Lisby M, Branzei D, Pfander B (2014) A cell cycle-regulated Slx4–Dpb11 complex promotes the resolution of DNA repair intermediates linked to stalled replication. *Genes Dev* 28: 1604–1619
- Hardy CF, Dryga O, Seematter S, Pahl PM, Sclafani RA (1997) mcm5/cdc46-bob1 bypasses the requirement for the S phase activator Cdc7p. *Proc Natl Acad Sci USA* 94: 3151–3155
- Heyer W-D, Ehmsen KT, Liu J (2010) Regulation of homologous recombination in eukaryotes. *Annu Rev Genet* 44: 113–139
- Ho CK, Mazón G, Lam AF, Symington LS (2010) Mus81 and Yen1 promote reciprocal exchange during mitotic recombination to maintain genome integrity in budding yeast. *Mol Cell* 40: 988–1000
- Interthal H, Heyer WD (2000) MUS81 encodes a novel helix-hairpin-helix protein involved in the response to UV- and methylation-induced DNA damage in *Saccharomyces cerevisiae*. *Mol Gen Genet* 263: 812–827
- Ip SCY, Rass U, Blanco MG, Flynn HR, Skehel JM, West SC (2008) Identification of Holliday junction resolvases from humans and yeast. *Nature* 456: 357–361
- Li X, Liu K, Li F, Wang J, Huang H, Wu J, Shi Y (2012) Structure of C-terminal tandem BRCT repeats of Rtt107 protein reveals critical role in interaction with phosphorylated histone H2A during DNA damage repair. *J Biol Chem* 287: 9137–9146
- Lopez-Mosqueda J, Maas NL, Jonsson ZO, DeFazio-Eli LG, Wohlschlegel J, Toczyski DP (2010) Damage-induced phosphorylation of Sld3 is important to block late origin firing. *Nature* 467: 479–483
- Lyons NA, Fonslow BR, Diedrich JK, Yates JR, Morgan DO (2013) Sequential primed kinases create a damage-responsive phosphodegron on Eco1. *Nat Struct Mol Biol* 20: 194–201
- Mankouri HW, Huttner D, Hickson ID (2013) How unfinished business from S-phase affects mitosis and beyond. *EMBO J* 32: 2661–2671
- Masai H, Taniyama C, Ogino K, Matsui E, Kakusho N, Matsumoto S, Kim JM, Ishii A, Tanaka T, Kobayashi T, Tamai K, Ohtani K, Arai K-I (2006) Phosphorylation of MCM4 by Cdc7 kinase facilitates its interaction with Cdc45 on the chromatin. *J Biol Chem* 281: 39249–39261
- Mathiasen DP, Lisby M (2014) Cell cycle regulation of homologous recombination in *Saccharomyces cerevisiae*. *FEMS Microbiol Rev* 38: 172–184
- Matos J, Lipp JJ, Bogdanova A, Guillot S, Okaz E, Junqueira M, Shevchenko A, Zachariae W (2008) Dbf4-dependent CDC7 kinase links DNA replication to the segregation of homologous chromosomes in meiosis I. *Cell* 135: 662–678
- Matos J, Blanco MG, Maslen S, Skehel JM, West SC (2011) Regulatory control of the resolution of DNA recombination intermediates during meiosis and mitosis. *Cell* 147: 158–172
- Matos J, Blanco MG, West SC (2013) Cell-cycle kinases coordinate the resolution of recombination intermediates with chromosome segregation. *Cell Rep* 4: 76–86
- Matos J, West SC (2014) Holliday junction resolution: regulation in space and time. *DNA Repair (Amst)* 19: 176–181
- Miller CT, Gabrielse C, Chen Y-C, Weinreich M (2009) Cdc7p-Dbf4p regulates mitotic exit by inhibiting polo kinase. *PLoS Genet* 5: 1–13
- Mok J, Kim PM, Lam HYK, Piccirillo S, Zhou X, Jeschke GR, Sheridan DL, Parker SA, Desai V, Jwa M, Cameroni E, Niu H, Good M, Remenyi A, Ma J-LN, Sheu Y-J, Sassi HE, Sopko R, Chan CSM, De Virgilio C et al (2010) Deciphering protein kinase specificity through large-scale analysis of yeast phosphorylation site motifs. *Sci Signal* 3: ra12
- Montagnoli A, Valsasina B, Brotherton D, Troiani S, Rainoldi S, Tenca P, Molinari A, Santocanale C (2006) Identification of Mcm2 phosphorylation sites by S-phase-regulating kinases. *J Biol Chem* 281: 10281–10290
- Montagnoli A, Valsasina B, Croci V, Menichincheri M, Rainoldi S, Marchesi V, Tibolla M, Tenca P, Brotherton D, Albanese C, Patton V, Alzani R, Ciavolella A, Sola F, Molinari A, Volpi D, Avanzi N, Fiorentini F, Cattoni M, Healy S et al (2008) A Cdc7 kinase inhibitor restricts initiation of DNA replication and has antitumor activity. *Nat Chem Biol* 4: 357–365
- Mortensen EM, Haas W, Gygi M, Gygi SP, Kellogg DR (2005) Cdc28-dependent regulation of the Cdc5/Polo kinase. *Curr Biol* 15: 2033–2037
- Muñoz IM, Hain K, Déclais A-C, Gardiner M, Toh GW, Sanchez-Pulido L, Heuckmann JM, Toth R, Macartney T, Eppink B, Kanaar R, Ponting CP, Lilley DMJ, Rouse J (2009) Coordination of structure-specific nucleases by human SLX4/BTBD12 is required for DNA repair. *Mol Cell* 35: 116–127
- Ohouo PY, de Oliveira FMB, Almeida BS, Smolka MB (2010) DNA damage signaling recruits the Rtt107-Slx4 scaffolds via Dpb11 to mediate replication stress response. *Mol Cell* 39: 300–306
- Ohouo PY, de Oliveira FMB, Liu Y, Ma CJ, Smolka MB (2012) DNA-repair scaffolds dampen checkpoint signalling by counteracting the adaptor Rad9. *Nature* 493: 120–124
- Pfander B, Diffley JFX (2011) Dpb11 coordinates Mec1 kinase activation with cell cycle-regulated Rad9 recruitment. *EMBO J* 30: 4897–4907
- Princz LN, Gritenaite D, Pfander B (2015) The Slx4–Dpb11 scaffold complex: coordinating the response to replication fork stalling in S-phase and the subsequent mitosis. *Cell Cycle* 14: 488–494
- Randell JCW, Fan A, Chan C, Francis LI, Heller RC, Galani K, Bell SP (2010) Mec1 is one of multiple kinases that prime the Mcm2–7 helicase for phosphorylation by Cdc7. *Mol Cell* 40: 353–363
- Saugar I, Vazquez MV, Gallo-Fernandez M, Ortiz-Bazan MA, Segurado M, Calzada A, Tercero JA (2013) Temporal regulation of the Mus81–Mms4 endonuclease ensures cell survival under conditions of DNA damage. *Nucleic Acids Res* 41: 8943–8958
- Schwartz EK, Wright WD, Ehmsen KT, Evans JE, Stahlberg H, Heyer WD (2012) Mus81–Mms4 functions as a single heterodimer to cleave nicked intermediates in recombinational DNA repair. *Mol Cell Biol* 32: 3065–3080

- Shirayama M, Zachariae W, Ciosk R, Nasmyth K (1998) The Polo-like kinase Cdc5p and the WD-repeat protein Cdc20p/fizzy are regulators and substrates of the anaphase promoting complex in *Saccharomyces cerevisiae*. *EMBO J* 17: 1336–1349
- Snead JL, Sullivan M, Lowery DM, Cohen MS, Zhang C, Randle DH, Taunton J, Yaffe MB, Morgan DO, Shokat KM (2007) A coupled chemical-genetic and bioinformatic approach to polo-like kinase pathway exploration. *Chem Biol* 14: 1261–1272
- Suzuki K, Sako K, Akiyama K, Isoda M, Senoo C, Nakajo N, Sagata N (2015) Identification of non-Ser/Thr-Pro consensus motifs for Cdk1 and their roles in mitotic regulation of C2H2 zinc finger proteins and Ect2. *Sci Rep* 5: 7929
- Svensden JM, Smogorzewska A, Sowa ME, O'Connell BC, Gygi SP, Elledge SJ, Harper JW (2009) Mammalian BTBD12/SLX4 assembles a Holliday junction resolvase and is required for DNA repair. *Cell* 138: 63–77
- Szakal B, Branzei D (2013) Premature Cdk1/Cdc5/Mus81 pathway activation induces aberrant replication and deleterious crossover. *EMBO J* 32: 1155–1167
- Weinreich M, Stillman B (1999) Cdc7p-Dbf4p kinase binds to chromatin during S phase and is regulated by both the APC and the RAD53 checkpoint pathway. *EMBO J* 18: 5334–5346
- Wyatt HDM, Sarbajna S, Matos J, West SC (2013) Coordinated actions of SLX1-SLX4 and MUS81-EME1 for Holliday junction resolution in human cells. *Mol Cell* 52: 234–247
- Zegerman P, Diffley JFX (2010) Checkpoint-dependent inhibition of DNA replication initiation by Sld3 and Dbf4 phosphorylation. *Nature* 467: 474–478



**License:** This is an open access article under the terms of the Creative Commons Attribution-NonCommercial-NoDerivs 4.0 License, which permits use and distribution in any medium, provided the original work is properly cited, the use is non-commercial and no modifications or adaptations are made.

## Expanded View Figures

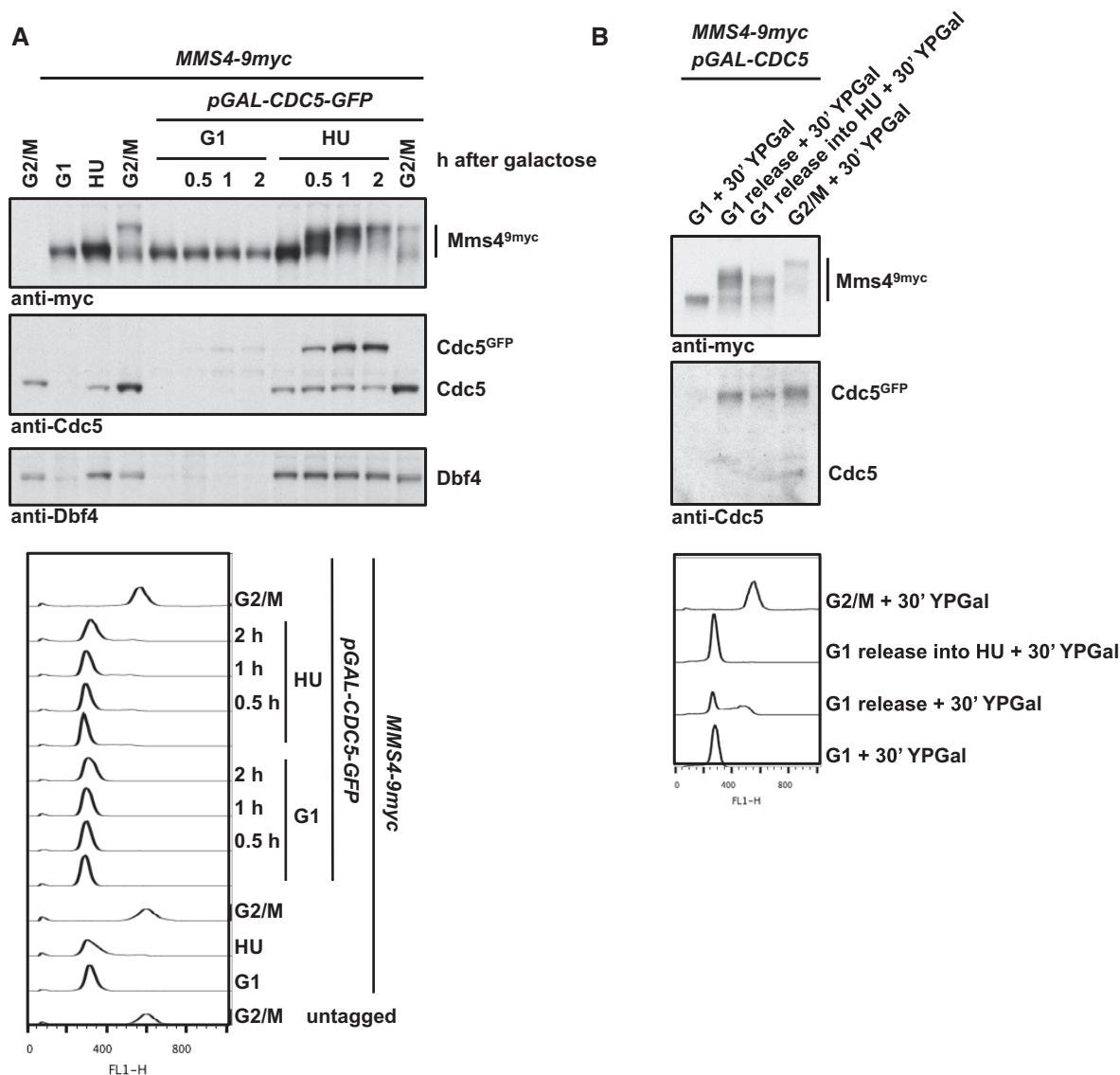


**Figure EV1. Cdc5 restricts Mms4 hyperphosphorylation to mitosis.**

- A** Overexpression of *CDC5* in S phase results in premature Mms4 hyperphosphorylation. Western blot analysis of Mms4<sup>9myc</sup>, Cdc5 and Dbf4 from whole-cell extracts (upper panel) and FACS data (lower panel). Cells were arrested in G1 (with alpha-factor), S phase (with HU) or G2/M phase (with nocodazole). After arrest, *CDC5<sup>GFP</sup>* overexpression was induced by addition of 2% galactose for the indicated time to cells harbouring an additional copy of GFP-tagged *CDC5* under the *GAL1* promoter. Samples were run in 7% Tris-acetate gels.
- B** Mms4 hyperphosphorylation by *CDC5* overexpression in S phase is reduced in HU-treated cells. Western blot analysis of Mms4<sup>9myc</sup> and Cdc5 from precipitated whole-cell extracts (upper panel) and FACS data (lower panel) of cells arrested in G1 (with alpha factor) or G2/M phase (with nocodazole), or released to S phase (with or without HU). *CDC5<sup>GFP</sup>* overexpression was induced for 30 min by addition of 2% galactose to cells harbouring an additional copy of GFP-tagged *CDC5* under the *GAL1* promoter. Note that upon *CDC5* overexpression cells are partially defective in bulk replication. Samples were run in 7% Tris-acetate gels.

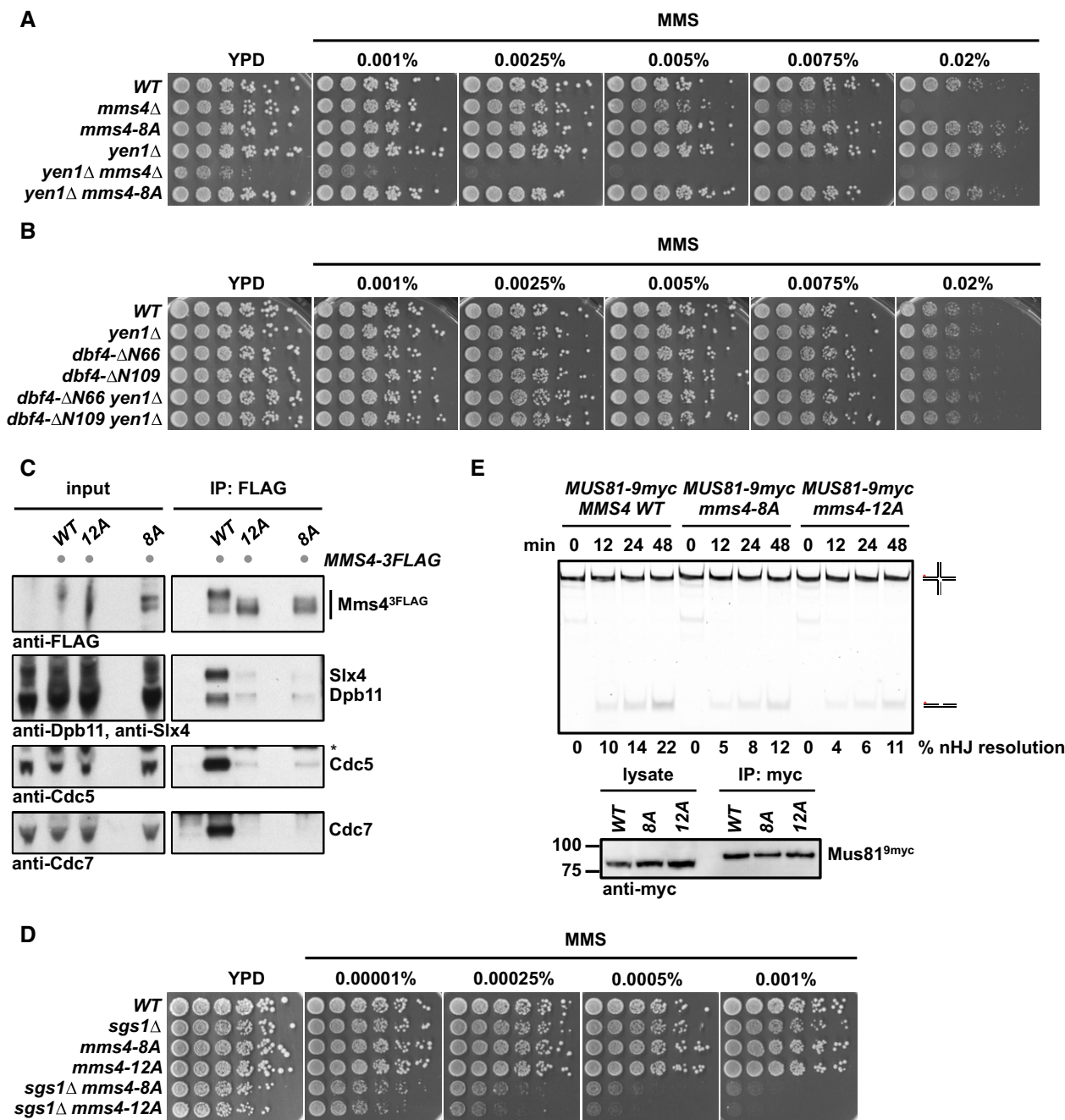


**Figure EV2. Phenotypic analysis of Mms4 variants deficient in (S/T)(S/T) phosphorylation sites.**

A, B The *mms4-8A* mutation or lack of Cdc5-DDK interaction does not lead to a synthetic hypersensitivity towards MMS in the *yen1*Δ background. Spotting assay as in Fig 4D and E.

C–E Additional mutation of 4 additional (S/T)(S/T) motifs in the background of the *mms4-8A* mutant (*mms4-12A*) leads to a reduction in the Mms4 phosphorylation shift (C), increases the hypersensitivity to MMS in the *sgs1*Δ background (D) and shows a slightly but not significantly decreased activity of Mus81–Mms4 (E). (C) Mms4<sup>3FLAG</sup> pull down as in Fig 1A, but in G2/M-arrested cells in untagged, WT, *mms4-12A* and *mms4-8A* backgrounds. Asterisk marks a cross-reactive band. (D) Spotting assay as in Fig 4D and E. (E) Resolution assay using a nHJ substrate and Mus81<sup>9myc</sup>–Mms4<sup>3FLAG</sup> purified from mitotically arrested WT, *mms4-8A* or *mms4-12A* cells. Lower panel: Western blot samples of anti-myc IPs.

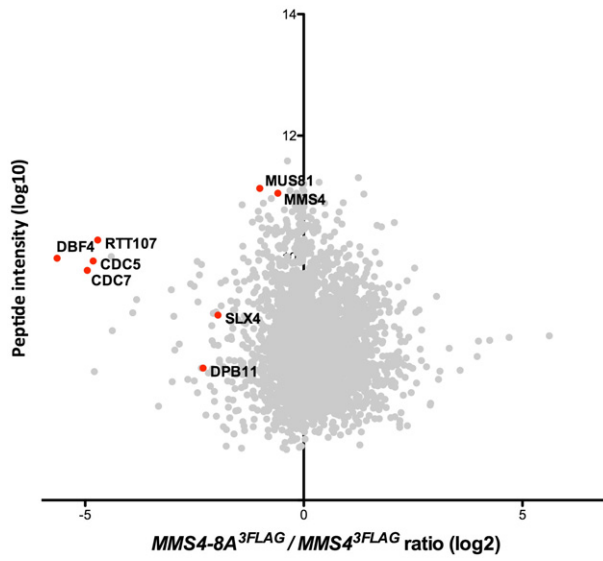


**Figure EV3.** A defect in the phosphorylation of Mms4 (S/T)(S/T) sites (*mms4-8A*) causes reduced association of Cdc5, DDK and Rtt107 with Mus81-Mms4.

SILAC-based quantification of Mms4<sup>3FLAG</sup> pull downs in WT vs. *mms4-8A* cells. Plotted are the H/L ratios against peptide intensity

## **Appendix – Table of Contents**

- **Appendix Figure Legends**
- **Appendix Figures**
- **Appendix Table S1**
- **Appendix Supplementary Materials and Methods (including Appendix Table S2)**
- **Appendix References**

## Appendix Figure Legends:

### Figure S1:

Mus81-Mms4 forms a complex in mitosis with kinases and scaffold proteins, and is a target to phosphorylation by these kinases.

**(A)** SILAC-based quantification of Mms4<sup>3FLAG</sup> pulldowns in untagged vs *MMS4*<sup>3FLAG</sup> cells after G2/M arrest with nocodazole. H/L ratios from two label-switch experiments without ratio count cut-off are plotted. #, as the only protein of the analysis Dpb11 displayed exclusively peptides that were derived from the Mms4<sup>3FLAG</sup> IP samples, but not the control samples. This experiment is already shown as Fig. S8A in Gritenaite *et al.*, 2014.

**(B)** Coomassie staining to show running behaviour of peptides used in Fig. 1C. Peptides 1-3 shift down upon increasing phosphorylation, whereas peptides 4-6 display an up-shift.

**(C)** Kinetic *in vitro* kinase assay. Purified, immobilized Mus81-Mms4 is either mock treated or treated with CDK in a non-radioactive priming step, and incubated with purified DDK (upper panel) or Cdc5 (lower panel). Samples were taken after indicated time points.

**(D)** Mus81-Mms4 *in vitro* phosphorylation is independent of DDK and/or CDK pre-phosphorylation. Purified, immobilized Mus81-Mms4 is incubated in an *in vitro* kinase assay with purified CDK2/cycA<sup>N170</sup> (a model CDK), DDK or Cdc5 (lanes 1-4). Additionally, Mus81-Mms4 is incubated with respective kinases after a non-radioactive priming step with DDK (lanes 5-8) or CDK and DDK (lanes 9-12).

### Figure S2:

DDK and Cdc5 target Mus81-Mms4 in an interdependent manner.

**(A)** Formation of the Mus81-Mms4 complex depends on Cdc5 activity. SILAC-based quantification of Mms4<sup>3FLAG</sup> pulldowns in *WT* vs *cdc5-as1* cells after mitotic arrest with nocodazole and additional treatment with 15  $\mu$ M CMK for 1 h. Plotted are the H/L ratios of two label-switch experiments.

**(B)** CDK activity is required for Mms4 hyperphosphorylation. Whole-cell extracts of *WT* and *cdc28-as1* cells arrested in mitosis, titrated with 1NM-PP1 as indicated.

**(C)** Phosphorylation shift of Mms4 in whole-cell extracts of mitotically arrested *WT* and mutant cells.

**(D)** Cdc5 association with Mus81-Mms4 is dependent on DDK activity. Mms4<sup>3FLAG</sup> pulldown as in Fig. 1A. Cells were cultivated and arrested in mitosis at RT. Inhibition of

DDK was achieved by using the *cdc7-1* allele and shifting cells to permissive temperature (38 °C) for the indicated time.

**(E)** Effect of DDK and Cdc5 mutants on Cdc5 substrates. Phosphorylation of Cdc5 substrates Ulp2 and Scc1 (and as control Mms4) was tested, indicated by their phosphorylation shift in 7% Tris-Acetate gels in untagged, *WT*, *cdc5-as1* and *cdc7Δ* backgrounds. Western blot analysis of Ulp2<sup>9myc</sup> and Scc1<sup>9myc</sup> whole-cell extracts from alpha-factor- (G1) or nocodazole-arrested (G2/M) cells. Cdc5 was inhibited by treatment with 15 μM CMK for 1 h.

**(F)** DDK and Cdc5 association to Mus81-Mms4 is reduced when the DNA damage checkpoint is triggered by DNA damage induction. Mms4<sup>3FLAG</sup> pulldown as in Fig. 1A, but in G2/M-arrested cells that were untreated or treated with 50 μg/ml phleomycin.

### **Figure S3:**

Summary of Mms4 phosphorylation sites. Shown is the Mms4 primary amino acid sequence. Colours indicate phosphorylation sites on endogenous Mms4 that were affected in SILAC-based mass spectrometry experiments (Fig. 3A-B) by Cdc5 inhibition (blue), *CDC7* deletion (red) or in both backgrounds (green). Serine to alanine exchanges in the *mms4-8A* mutant are boxed. Additional serine to alanine exchanges in the *mms4-12A* mutant are boxed with a dashed line.

### **Figure S4:**

DDK phosphorylation controls activation of Mus81-Mms4 resolvase activity in mitosis.

**(A)** Endogenous Mus81<sup>3FLAG</sup>-Mms4 purified from mitotically arrested cells shows increased activity compared to non-phosphorylated recombinant protein expressed in yeast. Left panel: Western blot analysis for quantification of bead-bound protein levels of Mus81 (endogenous and recombinant) compared to increasing amounts of soluble recombinant Mus81. Approx. 5 fmol Mus81<sup>3FLAG</sup>-Mms4 are used in the assay to cleave 500 fmol nHJ substrate. Right panel: Resolution assay using a nicked HJ substrate and comparing Mus81<sup>3FLAG</sup>-Mms4 purified from mitotically arrested cells with recombinant, dephosphorylated Mus81<sup>3FLAG</sup>-Mms4 in similar protein concentration.

**(B,C)** Interaction of Mus81-Mms4 with other complex factors such as Rtt107 and Cdc5 is salt-labile, but their absence does not influence Mus81-Mms4 activity.

**(B)** Mms4<sup>3FLAG</sup> pulldown as in Fig. 1A from mitotically arrested cells, but proteins were washed on beads with either low salt (150 mM NaCl) or high salt buffer (350 mM NaCl).

**(C)** Left panel: Resolution assay using a nHJ substrate and Mus81<sup>9myc</sup>-Mms4<sup>3FLAG</sup> purified from mitotically arrested cells under low salt (150 mM NaCl) or high salt (350 mM NaCl) conditions. Right panel: Western blots samples of anti-myc IPs.

**(D,F)** Western blot analysis of Mus81<sup>9myc</sup> IP samples that were used as inputs for the *in vitro* resolution assays of Fig. 4A and C, respectively.

**(E)** DDK is required for mitotic activation of Mus81-Mms4. Resolution assay using a replication fork (RF) substrate and Mus81<sup>9myc</sup>-Mms4<sup>3FLAG</sup> purified from mitotically arrested *bob1-1 (DDK+)* and *bob1-1 cdc7Δ* strains or untagged control cells. Lower panel: Western blots samples of anti-myc IPs.

### **Figure S5:**

Dpb11 interacts with the N-terminal region of Mms4 and its binding is dependent on CDK activity.

**(A)** Dpb11 binds to a minimal interacting fragment of Mms4 comprising the residues 101-230. Two-hybrid analysis of GAL4-BD fused to Dpb11 and GAL4-AD fusions with Mms4 or Mms4 fragment constructs (left panel). Expression of constructs was verified by western blot analysis (right panel).

**(B)** CDK activity is required for Dpb11 and Slx4 association with Mus81-Mms4. Mms4<sup>3FLAG</sup> pulldown as in Fig. 1A, but in G2/M-arrested *WT* and *cdc28-as1* mutant cells treated with 5 μM 1NM-PP1 for 1 h. This figure is from the same experiment as Fig. 2B and therefore as control includes the identical anti-Flag western.

**(C)** A defect in the Dpb11-Mms4 interaction introduces only a minor defect in Mus81 activation. Resolution assay using a nicked HJ substrate and Mus81<sup>9myc</sup>-Mms4<sup>3FLAG</sup> purified from mitotically arrested *WT* or *mms4-S201A* cells. Right panel: Western blots samples of anti-myc IPs.

### **Figure S6:**

The Rtt107 scaffold tethers DDK and Cdc5 to Mus81-Mms4.

**(A)** Formation of the Mus81-Mms4 complex depends on Rtt107. SILAC-based quantification of Mms4<sup>3FLAG</sup> pulldowns in *WT* vs *rtt107Δ* cells. Plotted are the H/L ratios of two experiments including label-switch.

**(B)** Rtt107 binding to Cdc5 and DDK is not affected by the presence of Mus81-Mms4. Rtt107<sup>3FLAG</sup> pulldown as in Fig. 1A, but in G2/M-arrested *WT* and *mus81Δ* cells.

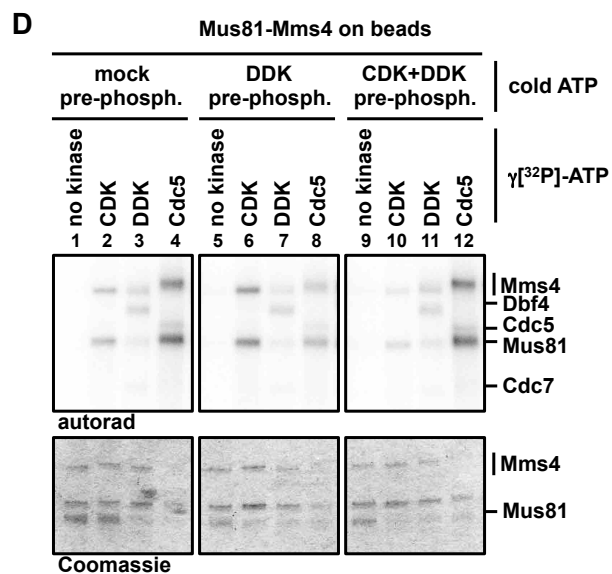
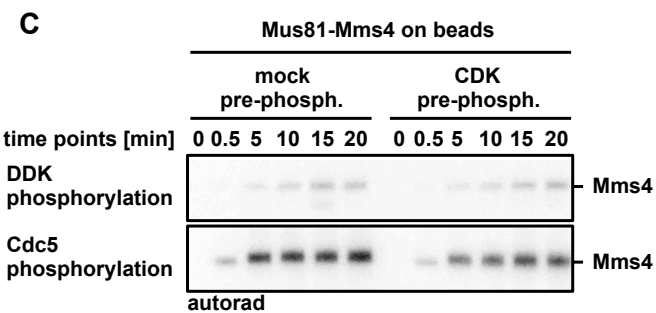
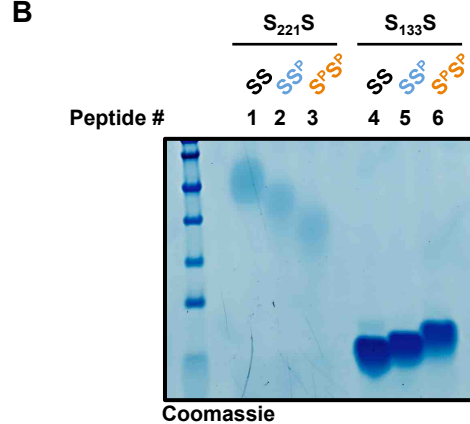
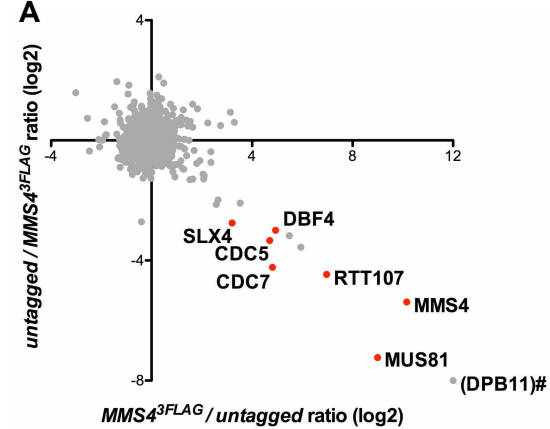
### **Figure S7:**

Rtt107 is required for efficient Mus81-Mms4 activation in mitosis.

**(A,B)** *Rtt107* influences the phosphorylation of specific Cdc5-dependent phosphorylation sites. SILAC-based MS analysis of Mms4 phosphorylation after purification of endogenously expressed Mus81-Mms4<sup>3FLAG</sup> **(A)** or of Mus81<sup>3FLAG</sup>-Mms4<sup>His10-Strep2</sup> expressed from the *pGAL1-10* promoter **(B)**.

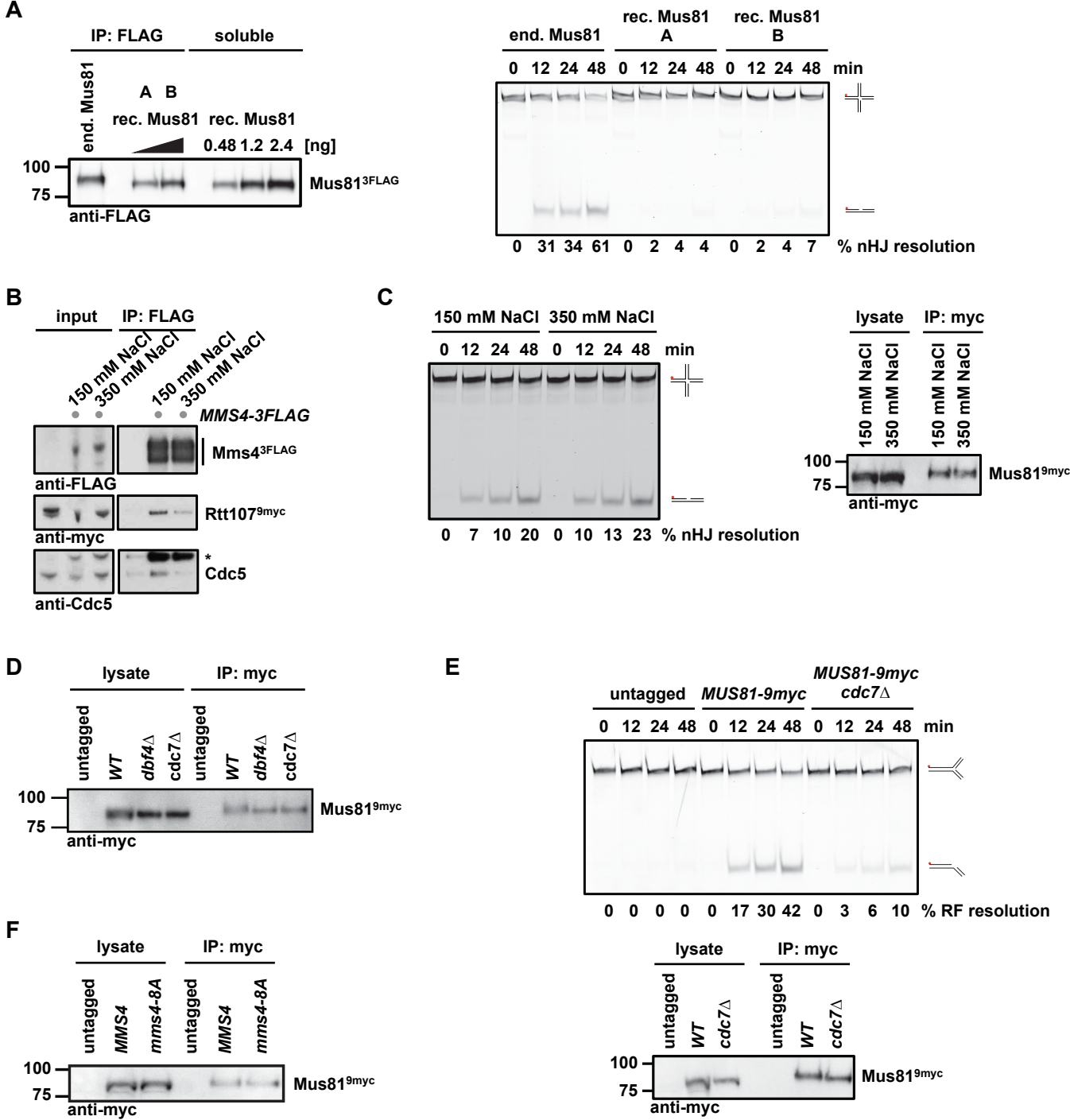
**(C)** Western blot analysis of Mus81<sup>9myc</sup> IP samples that were used as inputs for the *in vitro* for resolution assay of Fig. 7A.

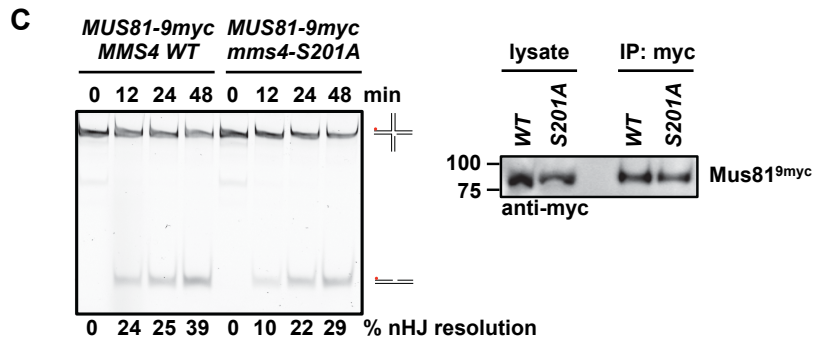
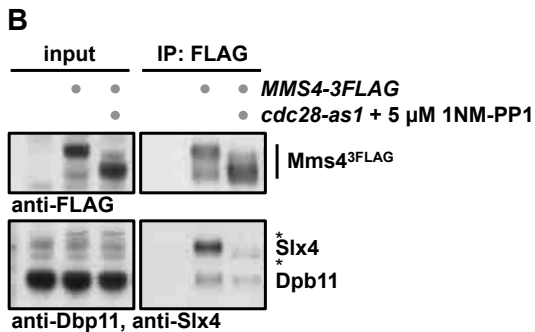
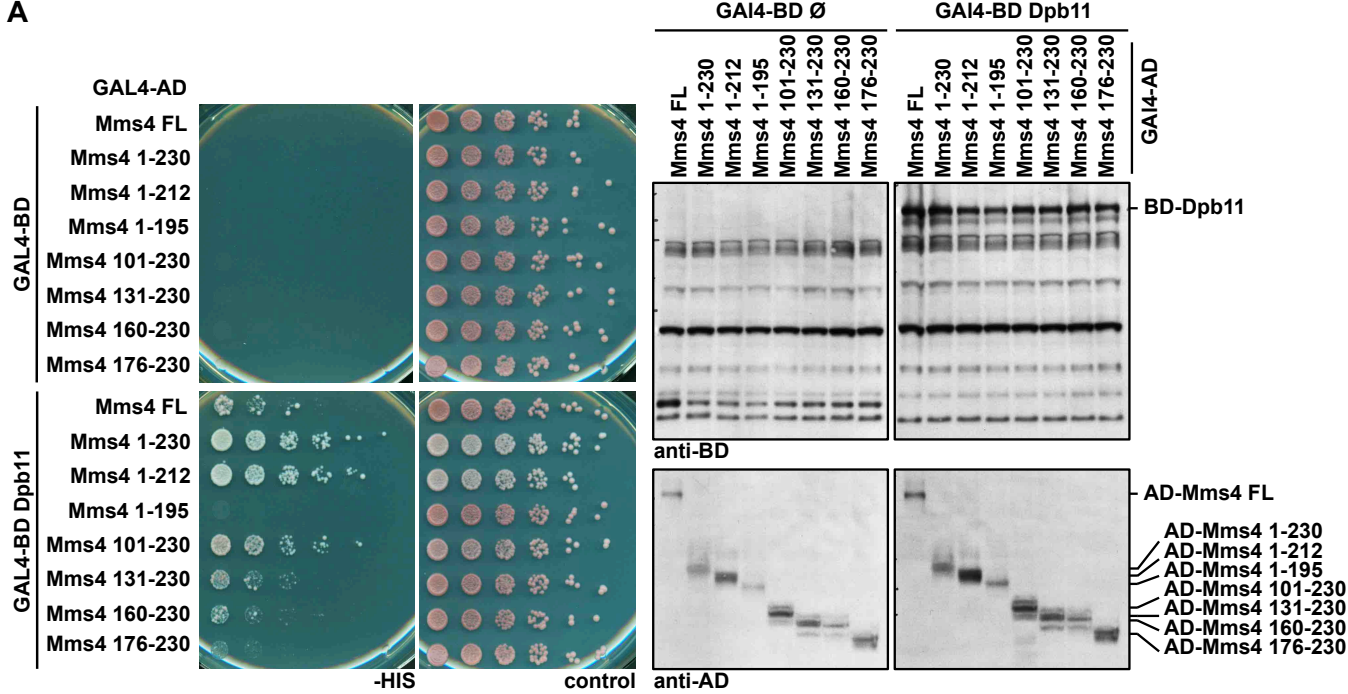
**(D)** *RTT107* deletion does not lead to a further reduction in Mus81 activity in the *cdc7Δ* background. Resolution assay using a nicked HJ substrate and Mus81<sup>9myc</sup>-Mms4<sup>3FLAG</sup> purified from mitotically arrested *bob1-1 cdc7Δ* or *bob1-1 cdc7Δ rtt107Δ* cells. Lower panel: Western blots samples of anti-myc IPs.

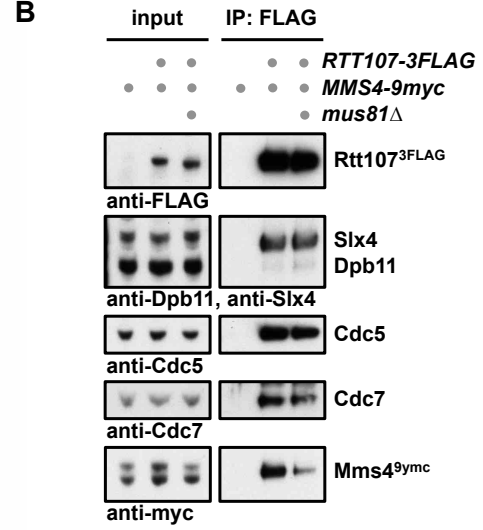
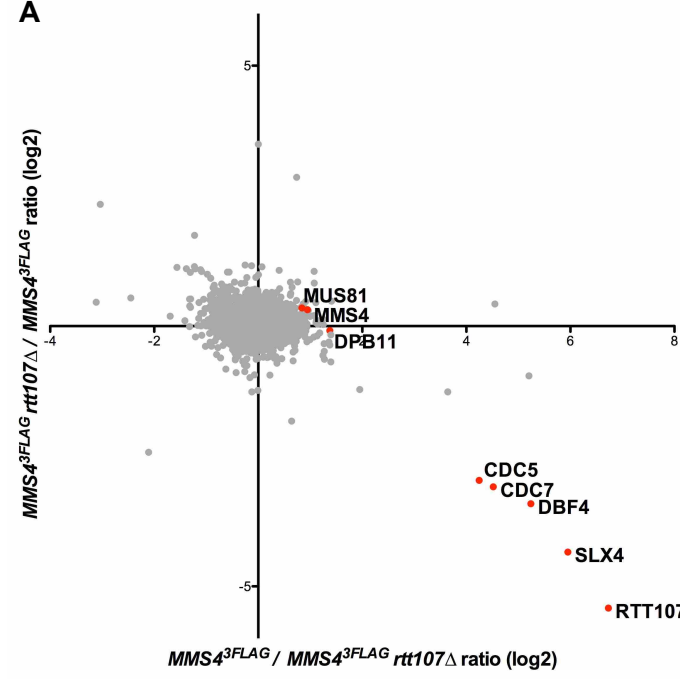




	10	20	30	40	50	60	70	80	90									
MSQIVDFVED	KDSRNDASIQ	IIDGSPSNVEI	IALSESMDQD	ECKRAHV	S	SA	EMIF	S	S	PQRK	SVSNDVENVD	LNKSIELSAP	FFQDISISKL	DDF	S	T	VNSI	100
IF	S	SLRNENN	AKGNAKLLD	DLISDEWSAD	LE	S	S	SGKKHKNK	SQYNLRDIAE	KWGVQSLKNP	EPIAVDCEYK	TQGIGKTNSD	ISDSPKSQIG	AADILDFDPL				200
SPVKHENP	T	E	EKHNSIANEN	S	S	P	D	NSLKPA	GKQNHGEDG	T	S	MAKRVYKNG	EDEQEHLPGK	KKRTIAL	S	R	T	300
S	T	PAKGSNIV	RTGSQPIFSN	ANCFQEAQRS	KT	L	T	AEDPKC	TKNTAREV	S	Q	LENYIAYGQY	YTREDSKNKI	RHLLKENKNA	FKRVNQIYRD	NIKARSQMII		400
EFSPSLLQLF	KKGDSDLQQQ	LAPAVVQ	S	S	Y	NDSMPLLRFL	RKCD	SIYDFS	NDFYYP	CDPK	IVEENVLILY	YDAQEFFEQY	TSQKKELYRK	IRFFSKNGKH				500
VILILSDINK	LKRAIFQLEN	EKYKARVEQR	L	S	G	T	E	EALRP	RSK	K	S	S	Q	V	G	K	L	600
AIRYMKY AHL	NVKS	Q	D	S	T	E	TLKKT	FHQIG	RMPEMKANNV	VSLYPSFQSL	LEDIEKGRLO	SDNEGKYLMT	EAVEKRLYKL	FTCTDPNDTI	E.			700









**Appendix Table S1. Mms4 phosphorylation sites and their regulation by DDK or Cdc5 as detected by SILAC-based quantitative mass spectrometry (Fig. 3)**

Mus81-Mms4 endogenous	Mus81-Mms4 overexpressed
2	2
48	48
49	49
55	55
56	56
61	61
63	63
74	74
86	78**
88*	86
94**	88**
96	94
99	95
103	96
104	99
124**	103
128**	104
133**	124
134**	128
141**	133
156**	134
184*	141
187	156
201	187
209**	201
221*	222*
222*	264
240**	268
241**	274*
268**	280*
286	286
291	291
292	292
294	294
296**	297
297**	301
301	302
302	314
314**	330**
330**	349
349	366
366**	396**
396**	532
532	542

\* not measured in *cdc5-as1*

\*\* not measured in *cdc7Δ*

phosphorylation sites affected in *cdc5-as1*

phosphorylation sites affected in *cdc7Δ*

phosphorylation sites affected in *cdc5-as1* and *cdc7Δ* backgrounds

## Appendix Supplementary Materials and Methods

### Yeast strains and construction

All yeast strains are based on W303 (Thomas & Rothstein, 1989). Genotypes are listed below. All biochemical experiments were performed in a W303-1A *pep4*Δ background. The genetic experiments in Fig. 4D-E, 5C, and EV2A,B,D were performed in a W303 *RAD5+* background to exclude any effect from a partial defect of the *rad5-535* allele. Two-hybrid analyses were performed in the strain PJ69-7A (James *et al.*, 1996).

*S. cerevisiae* strains were prepared by genetic crosses and transformation techniques. Deletion of particular genes and endogenous protein tagging were performed as described (Knop *et al.*, 1999). Correct integrations were checked by genotyping PCR. Denaturing cell extracts were prepared by alkaline lysis and TCA precipitation. The *mms4* alleles were generated using site-directed mutagenesis and integrated as linear plasmids at the TRP1 locus.

**Appendix Table S2. Yeast strains used in this study**

Strain	Full genotype	Relevant genotype	Source
MGBY3294	MATa <i>ade2-1 his3-11 leu2-3,112 trp1Δ2 can1-100 pep4::KanMX bar1::hph-NT1 ura3-52::GAL1,10p-FLAG3-MUS81/GST-His10-Strep2-MMS4::URA3</i>	<i>pGAL-FLAG3-MUS81-GST-His10-Strep2-MMS4</i>	This study (Blanco lab)
YBP388	MATa <i>ade2-1 ura3-1 his3-11,15 trp1-1 can1-100 leu2-3,112::pep4::LEU2</i>	<i>pep4</i>	Klein lab
YDG208	MATa <i>RAD5+ ade2-1 ura3-1 leu2-3,112 his3-11,15 trp1-1 can1-100</i>		This study
YDG291	MATa <i>RAD5+ ade2-1 ura3-1 leu2-3,112 his3-11,15 trp1-1 can1-100 yen1::hph-NT1</i>	<i>yen1</i>	Gritenaite et al., 2014
YDG329	MATa <i>RAD5+ ade2-1 ura3-1 leu2-3,112 his3-11,15 trp1-1 can1-100 sgs1::hph-NT1</i>	<i>sgs1</i>	Gritenaite et al., 2014
YDG355	MATa <i>RAD5+ ade2-1 ura3-1 his3-11,15 trp1-1 can1-100 mms4::hph-NT1 leu2-3,112::mms4-SS184,201AA::LEU2</i>	<i>mms4-SS184,201AA</i>	Gritenaite et al., 2014
YDG356	MATa <i>RAD5+ ade2-1 ura3-1 trp1-1 can1-100 mms4::hph-NT1 leu2-3,112::mms4-SS184,201AA::LEU2 his3-11,15::sgs1::HIS3Mx4</i>	<i>mms4-SS184,201AA sgs1</i>	Gritenaite et al., 2014
YDG376	MATa <i>RAD5+ ade2-1 ura3-1 leu2-3,112 his3-11,15 trp1-1 can1-100 yen1::hph-NT1 sgs1::nat-NT2</i>	<i>yen1 sgs1</i>	Gritenaite et al., 2014

YJB82	Mata/Matalpha <i>ade2-1/ade2-1 ura3-1/ura3-1 leu2-3,112/leu2-3,112 his3-11,15/his3-11,15 trp1-1/trp1-1 can1-100/can1-100 ade2-n/ade2-I LYS2/lys2::Gal-ISceI his3::NATMX/his3::HPHMX4 met22::kIURA3/MET22</i>	<i>diploid</i>	This study
YJB84	Mata/Matalpha <i>ade2-1/ade2-1 ura3-1/ura3-1 leu2-3,112/leu2-3,112 his3-11,15/his3-11,15 trp1-1/trp1-1 can1-100/can1-100 ade2-n/ade2-I LYS2/lys2::Gal-ISceI his3::NATMX/his3::HPHMX4 met22::kIURA3/MET22 rtt107::KanMX/rtt107::KanMX</i>	<i>diploid rtt107</i>	This study
YJB86	Mata/Matalpha <i>ade2-1/ade2-1 ura3-1/ura3-1 leu2-3,112/leu2-3,112 his3-11,15/his3-11,15 trp1-1/trp1-1 can1-100/can1-100 ade2-n/ade2-I LYS2/lys2::Gal-ISceI his3::NATMX/his3::HPHMX4 met22::kIURA3/MET22 mms4::KanMX/mms4::KanMX trp1-1:pRS304-Mms4-SSSSSSS48,55,103,133,221,291,301,428AAA AAAAA:TRP1/trp1-1:pRS304-Mms4-SSSSSSS48,55,103,133,221,291,301,428AAA AAAAA:TRP1</i>	<i>diploid mms4-SSSSSSS48,55,103,133,221,291,301,428AAA AAAAA</i>	This study
YLP015	MATa <i>ade2-1 ura3-1 his3-11,15 can1-100 trp1-1::bar1::TRP1 leu2-3,112::pep4::LEU2 lys1::nat-NT2</i>	<i>lys1</i>	Gritenaite et al., 2014
YLP063	MATa <i>RAD5+ ade2-1 ura3-1 leu2-3,112 trp1-1 can1-100 cdc5-as1 his3-11,15::pep4::HIS3Mx4 MMS4-3FLAG::hph-NT1</i>	<i>MMS4-3FLAG cdc5-as1</i>	Gritenaite et al., 2014
YLP065	MATa <i>ade2-1 ura3-1 his3-11,15 can1-100 trp1-1::bar1::TRP1 leu2-3,112::pep4::LEU2 lys1::nat-NT2 MMS4-3FLAG::hph-NT1</i>	<i>lys1 MMS4-3FLAG</i>	This study
YLP070	MATa <i>ade2-1 ura3-1 leu2-3,112 can1-100 his3-11,15::pep4::HIS3Mx4 lys1::nat-NT2 mms4::KanMx trp1-1::mms4-S184A::TRP1 MMS4-3FLAG::hph-NT1</i>	<i>lys1 mms4-S184A-3FLAG</i>	This study
YLP074	MATa <i>ade2-1 ura3-1 leu2-3,112 can1-100 his3-11,15::pep4::HIS3Mx4 lys1::nat-NT2 mms4::KanMx trp1-1::mms4-S201A::TRP1 MMS4-3FLAG::hph-NT1</i>	<i>lys1 mms4-S201A-3FLAG</i>	This study
YLP078	MATa <i>ade2-1 ura3-1 leu2-3,112 trp1-1 can1-100 his3-11,15::pep4::HIS3Mx4 MMS4-3FLAG::hph-NT1 slx4::KanMx</i>	<i>MMS4-3FLAG slx4</i>	Gritenaite et al., 2014

YLP092	MATa <i>ade2-1 ura3-1 his3-11,15 trp1-1 can1-100 leu2-3,112::pep4::LEU2 RTT107-9myc::hph-NT1</i>	<i>RTT107-9myc</i>	This study
YLP100	MATa <i>ade2-1 ura3-1 trp1-1 leu2-3,112 can1-100 his3-11,15::bob1-1::HIS3Mx4 pep4::hph-NT1</i>	<i>bob1-1</i>	This study
YLP111	MATa <i>ade2-1 ura3-1 trp1-1 leu2-3,112 can1-100 his3-11,15::bob1-1::HIS3Mx4 pep4::hph-NT1 MMS4-3FLAG::KanMx4</i>	<i>bob1-1 MMS4-3FLAG</i>	This study
YLP113	MATa <i>ade2-1 ura3-1 trp1-1 leu2-3,112 can1-100 his3-11,15::bob1-1::HIS3Mx4 pep4::hph-NT1 cdc7::nat-NT2 MMS4-3FLAG::KanMx4</i>	<i>bob1-1 cdc7 MMS4-3FLAG</i>	This study
YLP121	MATa <i>RAD5+ ade2-1 ura3-1 leu2-3,112 trp1-1 can1-100 cdc5-as1 his3-11,15::pep4::HIS3Mx4 lys1::nat-NT2 MMS4-3FLAG::hph-NT1</i>	<i>lys1 MMS4-3FLAG cdc5-as1</i>	This study
YLP126	MATa <i>ade2-1 leu2-3,112 trp1-1 can1-100 his3-11,15::bob1-1::HIS3Mx4 pep4::hph-NT1 cdc7::nat-NT2 MMS4-3FLAG::KanMx4 ura3-1::lys1::URA3</i>	<i>lys1 bob1-1 cdc7 MMS4-3FLAG</i>	This study
YLP128	MATa <i>ade2-1 ura3-1 leu2-3,112 trp1-1 can1-100 his3-11,15::pep4::HIS3Mx4 cdc7-1</i>	<i>cdc7-1</i>	This study
YLP132	MATa <i>ade2-1 ura3-1 leu2-3,112 trp1-1 can1-100 his3-11,15::pep4::HIS3Mx4 cdc7-1 MMS4-3FLAG::KanMx</i>	<i>cdc7-1 MMS4-3FLAG</i>	This study
YLP156	MATa <i>ade2-1 ura3-1 leu2-3,112 trp1-1 can1-100 his3-11,15::pep4::HIS3Mx4 MMS4-3FLAG::hph-NT1 RTT107-9myc::nat-NT2</i>	<i>MMS4-3FLAG RTT107-9myc</i>	This study
YLP164	MATa <i>ade2-1 ura3-1 leu2-3,112 can1-100 MMS4-3FLAG::hph-NT1 his3-11,15::pep4::HIS3Mx4 rtt107::KanMx trp1-1::lys1::TRP1</i>	<i>lys1 MMS4-3FLAG rtt107</i>	This study
YLP277	MATa <i>ade2-1 ura3-1 trp1-1 leu2-3,112 can1-100 MMS4-3FLAG::hph-NT1 his3-11,15::pep4::HIS3Mx4 SCC1-9myc</i>	<i>MMS4-3FLAG SCC1-9myc</i>	This study
YLP279	MATa <i>RAD5+ ade2-1 ura3-1 trp1-1 leu2-3,112 can1-100 cdc5-as1 MMS4-3FLAG::hph-NT1 his3-11,15::pep4::HIS3 SCC1-9myc::KanMx</i>	<i>MMS4-3FLAG SCC1-9myc cdc5-as1</i>	This study
YLP287	MATa <i>ade2-1 ura3-1 leu2-3,112 can1-100 his3-11,15::pep4::HIS3Mx4 mms4::KanMx trp1-1::mms4-S201A::TRP1 MMS4-3FLAG::hph-NT1 RTT107-9myc::nat-NT2</i>	<i>mms4-S201A-3FLAG RTT107-9myc</i>	This study

YLP339	MATa <i>RAD5+ ade2-1 ura3-1 leu2-3,112 his3-11,15 can1-100 mms4::hph-NT1 trp1-1::mms4-SSSSSSSS48,55,103,133,221,291,301,428AAAAAAA::TRP1</i>	<i>mms4-SSSSSSSS48,55,103,133,221,291,301,428AAAAAAA</i>	This study
YLP341	MATa <i>RAD5+ ade2-1 ura3-1 leu2-3,112 his3-11,15 can1-100 mms4::hph-NT1 trp1-1::mms4-SSSSSSSS48,55,103,133,221,291,301,428AAAAAAA::TRP1 sgs1::nat-NT2</i>	<i>mms4-SSSSSSSS48,55,103,133,221,291,301,428AAAAAAA sgs1</i>	This study
YLP350	MATa <i>RAD5+ ade2-1 ura3-1 leu2-3,112 his3-11,15 can1-100 mms4::hph-NT1 trp1-1::mms4-SSSSSSSS48,55,103,133,221,291,301,428AAAAAAA::TRP1 yen1::KanMx</i>	<i>mms4-SSSSSSSS48,55,103,133,221,291,301,428AAAAAAA yen1</i>	This study
YLP351	MATa <i>RAD5+ ade2-1 ura3-1 leu2-3,112 his3-11,15 can1-100 mms4::hph-NT1 trp1-1::mms4-SSSSSSSS48,55,103,133,221,291,301,428AAAAAAA::TRP1 sgs1::nat-NT2 yen1::KanMx</i>	<i>mms4-SSSSSSSS48,55,103,133,221,291,301,428AAAAAAA sgs1 yen1</i>	This study
YLP344	MATa <i>ade2-1 ura3-1 leu2-3,112 trp1-1 can1-100 MMS4-3FLAG::hph-NT1 his3-11,15::pep4::HIS3Mx4 dbf4-ΔN66::KanMx</i>	<i>MMS4-3FLAG dbf4-ΔN66</i>	This study
YLP345	MATa <i>ade2-1 ura3-1 leu2-3,112 trp1-1 can1-100 MMS4-3FLAG::hph-NT1 his3-11,15::pep4::HIS3Mx4 dbf4-ΔN109::KanMx</i>	<i>MMS4-3FLAG dbf4-ΔN109</i>	This study
YLP356	MATa <i>ade2-1 ura3-1 leu2-3,112 can1-100 mms4::KanMx his3-11,15::pep4::HIS3 trp1-1::mms4-SSSSSSSS48,55,103,133,221,291,301,428AAAAAAA::TRP1 MMS4-3FLAG::hph-NT1</i>	<i>mms4-SSSSSSSS48,55,103,133,221,291,301,428AAAAAAA-3FLAG</i>	This study
YLP360	MATa <i>ade2-1 ura3-1 leu2-3,112 his3-11,15 trp1-1 can1-100 MMS4-3FLAG::hph-NT1 cdc28-as1</i>	<i>MMS4-3FLAG cdc28-as1</i>	This study
YLP367	MATa <i>ade2-1 ura3-1 leu2-3,112 can1-100 mms4::KanMx his3-11,15::pep4::HIS3Mx4 trp1-1:: MMS4::TRP1 MMS4-3FLAG::hph-NT1 MUS81-9myc::nat-NT2</i>	<i>MMS4-3FLAG MUS81-9myc</i>	This study

YLP368	MATa <i>ade2-1 ura3-1 leu2-3,112 can1-100 mms4::KanMx his3-11,15::pep4::HIS3Mx4 trp1-1::mms4-SSSSSSSS48,55,103,133,221,291,301,428AAAAAAA::TRP1 MMS4-3FLAG::hph-NT1 MUS81-9myc::nat-NT2</i>	<i>mms4-SSSSSSSS48,55,103,133,221,291,301,428AAAAAAA-3FLAG MUS81-9myc</i>	This study
YLP369	MATa <i>RAD5+ ade2-1 ura3-1 leu2-3,112 his3-11,15 trp1-1 can1-100 dbf4-ΔN66::KanMx</i>	<i>dbf4-ΔN66</i>	This study
YLP370	MATa <i>RAD5+ ade2-1 ura3-1 leu2-3,112 his3-11,15 trp1-1 can1-100 dbf4-ΔN109::KanMx</i>	<i>dbf4-ΔN109</i>	This study
YLP371	MATa <i>RAD5+ ade2-1 ura3-1 leu2-3,112 his3-11,15 trp1-1 can1-100 dbf4-ΔN66::KanMx sgs1::hph-NT1</i>	<i>dbf4-ΔN66 sgs1</i>	This study
YLP372	MATa <i>RAD5+ ade2-1 ura3-1 leu2-3,112 his3-11,15 trp1-1 can1-100 dbf4-ΔN109::KanMx sgs1::hph-NT1</i>	<i>dbf4-ΔN109 sgs1</i>	This study
YLP374	MATa <i>RAD5+ ade2-1 ura3-1 leu2-3,112 his3-11,15 trp1-1 can1-100 dbf4-ΔN66::KanMx yen1::hph-NT1</i>	<i>dbf4-ΔN66 yen1</i>	This study
YLP375	MATa <i>RAD5+ ade2-1 ura3-1 his3-11,15 trp1-1 leu2-3,112 can1-100 dbf4-ΔN109::KanMx yen1::hph-NT1</i>	<i>dbf4-ΔN109 yen1</i>	This study
YLP438	MATa <i>ade2-1 ura3-1 trp1-1 leu2-3,112 can1-100 MMS4-3FLAG::hph-NT1 his3-11,15::pep4::HIS3 ULP2-9myc::KanMx</i>	<i>MMS4-3FLAG ULP2-9myc</i>	This study
YLP439	MATa <i>RAD5+ ade2-1 ura3-1 trp1-1 leu2-3,112 can1-100 cdc5-as1 MMS4-3FLAG::hph-NT1 his3-11,15::pep4::HIS3 ULP2-9myc::KanMx</i>	<i>MMS4-3FLAG ULP2-9myc cdc5-as1</i>	This study
YLP442	MATa <i>ade2-1 ura3-1 leu2-3,112 can1-100 mms4::KanMx his3-11,15::pep4::HIS3 trp1-1::mms4-SSSSSSSS48,55,103,133,221,291,301,428AAAAAAA::TRP1 MMS4-3FLAG::hph-NT1 lys1::nat-NT2</i>	<i>lys1 mms4-SSSSSSSS48,55,103,133,221,291,301,428AAAAAAA-3FLAG</i>	This study
YLP444	MATa <i>ade2-1 ura3-1 leu2-3,112 can1-100 mms4::KanMx his3-11,15::pep4::HIS3 trp1-1::mms4- S201A::TRP1 MMS4-3FLAG::hph-NT1 MUS81-9myc::nat-NT2</i>	<i>mms4-S201A-3FLAG MUS81-9myc</i>	This study
YLP445	MATa <i>ade2-1 ura3-1 leu2-3,112 can1-100 trp1-1::MUS81-9myc::TRP1 his3-11,15::bob1-1::HIS3 pep4::hph-NT1 MMS4-3FLAG::KanMx cdc7::nat-NT2 rtt107::kiURA</i>	<i>bob1-1 MUS81-9myc cdc7 rtt107</i>	This study
YLP458	MATa <i>ade2-1 his3-11,15 can1-100 trp1-1::bar1::TRP1 leu2-3,112::pep4::LEU2 lys1::nat-NT2 ura3-1::pRS306-pGAL1,10-FLAG3-MUS81-His-Strep-MMS4::URA3</i>	<i>lys1 pGAL-FLAG3-MUS81-His10-Strep2-MMS4</i>	This study

YLP459	MATa <i>ade2-1 trp1-1 leu2-3,112 can1-100 his3-11,15::bob1-1::HIS3 pep4::hph-NT1 lys1::nat-NT2 ura3-1::pRS306-pGAL1,10-FLAG3-MUS81-His-Strep-MMS4::URA3</i>	<i>lys1 pGAL-FLAG3-MUS81-His10-Strep2-MMS4</i>	This study
YLP461	MATa <i>ade2-1 ura3-1 leu2-3,112 can1-100 mms4::KanMx his3-11,15::pep4::HIS3 trp1-1::mms4-SSSSSSSSSSSS48,55,94,103,133,221,274,291,301,428,545,618AAAAAAAAAAAAA::TRP1 MMS4-3FLAG::hph-NT1</i>	<i>mms4-SSSSSSSSSSSS48,55,94,103,133,221,274,291,301,428,545,618AAAAAAAAAAAAA-3FLAG</i>	This study
YLP462	MATa <i>RAD5+ ade2-1 ura3-1 leu2-3,112 his3-11,15 can1-100 mms4::hph-NT1 trp1-1::mms4-SSSSSSSSSSSS48,55,94,103,133,221,274,291,301,428,545,618AAAAAAAAAAAAA::TRP1</i>	<i>mms4-SSSSSSSSSSSS48,55,94,103,133,221,274,291,301,428,545,618AAAAAAAAAAAAA</i>	This study
YLP463	MATa <i>RAD5+ ade2-1 ura3-1 leu2-3,112 his3-11,15 can1-100 mms4::hph-NT1 trp1-1::mms4-SSSSSSSS48,55,94,103,133,221,274,291,301,428,545,618AAAAAAAAA::TRP1 sgs1::nat-NT2</i>	<i>mms4-SSSSSSSSSSSS48,55,94,103,133,221,274,291,301,428,545,618AAAAAAAAAAAAA sgs1</i>	This study
YLP465	MATa <i>ade2-1 ura3-1 leu2-3,112 can1-100 his3-11,15::bob1-1::HIS3Mx4 pep4::hph-NT1 cdc7::nat-NT2 MMS4-3FLAG::KanMx4 trp1-1::ULP2-9myc::TRP1</i>	<i>bob1-1 cdc7 MMS4-3FLAG ULP2-9myc</i>	This study
YLP466	MATa <i>ade2-1 ura3-1 leu2-3,112 can1-100 his3-11,15::bob1-1::HIS3Mx4 pep4::hph-NT1 cdc7::nat-NT2 MMS4-3FLAG::KanMx4 trp1-1::SCC1-9myc::TRP1</i>	<i>bob1-1 cdc7 MMS4-3FLAG SCC1-9myc</i>	This study
YLP468	MATa <i>ade2-1 ura3-1 leu2-3,112 can1-100 mms4::KanMx his3-11,15::pep4::HIS3 trp1-1::mms4-SSSSSSSSSSSS48,55,94,103,133,221,274,291,301,428,545,618AAAAAAAAAAAAA::TRP1 MMS4-3FLAG::hph-NT1 MUS81-9myc::nat-NT2</i>	<i>mms4-SSSSSSSSSSSS48,55,94,103,133,221,274,291,301,428,545,618AAAAAAAAAAAAA-3FLAG MUS81-9myc</i>	This study
YLP469	MATa <i>RAD5+ ade2-1 leu2-3,112 trp1-1 can1-100 cdc5-as1 his3-11,15::pep4::HIS3Mx4 lys1::nat-NT2 ura3-1::GAL1,10p-FLAG3-MUS81/His10-Strep2-MMS4::URA3</i>	<i>lys1 cdc5-as1 pGAL-FLAG3-MUS81-His10-Strep2-MMS4</i>	This study
YLP470	MATa <i>ade2-1 leu2-3,112 trp1-1 can1-100 his3-11,15::bob1-1::HIS3Mx4 pep4::hph-NT1 cdc7::KanMx lys1::nat-NT2 ura3-1::GAL1,10p-FLAG3-MUS81/His10-Strep2-MMS4::URA3</i>	<i>lys1 bob1-1 cdc7 pGAL-FLAG3-MUS81-His10-Strep2-MMS4</i>	This study

YLP471	MATa <i>ade2-1 his3-11,15 trp1-1 can1-100 leu2-3,112::pep4::LEU2 rtt107::KanMx lys1::nat-NT2 ura3-1::GAL1,10p-FLAG3-MUS81/His10-Strep2-MMS4::URA3</i>	<i>lys1 rtt107 pGAL-FLAG3-MUS81-His10-Strep2-MMS4</i>	This study
YML1601	MATa <i>his3Δ1 leu2Δ0 met15Δ0 ura3Δ0 ADE2 MMS4-9myc::KanMx trp1-1::pGAL1-CDC5-GFP::TRP1</i>	<i>MMS4-9myc pGAL-CDC5-GFP</i>	Matos et al., 2013
YML3304	MATa <i>ade2-1 ura3-1 leu2-3,112 can1-100 trp1-1::MUS81-9myc::TRP1 his3-11,15::bob1-1::HIS3 pep4::hph-NT1 MMS4-3FLAG::KanMx dbf4::nat-NT2</i>	<i>bob1-1 MUS81-9myc dbf4</i>	This study (Matos lab)
YML3306	MATa <i>ade2-1 ura3-1 leu2-3,112 can1-100 trp1-1::MUS81-9myc::TRP1 his3-11,15::bob1-1::HIS3 pep4::hph-NT1 MMS4-3FLAG::KanMx cdc7::nat-NT2</i>	<i>bob1-1 MUS81-9myc cdc7</i>	This study (Matos lab)
YML3447	MATa <i>ade2-1 ura3-1 leu2-3,112 can1-100 trp1-1::MUS81-9myc::TRP1 his3-11,15::bob1-1::HIS3 pep4::hph-NT1 MMS4-3FLAG::nat-NT2 rtt107::KanMx</i>	<i>bob1-1 MUS81-9myc rtt107</i>	This study (Matos lab)
YSS3	MATa <i>ade2-1 ura3-1 trp1-1 leu2-3,112 can1-100 MMS4-3FLAG::hph-NT1 his3-11,15::pep4::HIS3Mx4</i>	<i>MMS4-3FLAG</i>	Gritenaite et al., 2014
YFZ020	MATa <i>ade2-1 ura3-1 trp1-1 can1-100 his3-11,15::pRS303-CDC5-3FLAG-pGAL1-GAL4::HIS3Mx4 leu2-3,112::pep4::LEU2</i>	<i>pGAL-CDC5-3FLAG</i>	This study
YFZ021	MATa <i>ade2-1 ura3-1 trp1-1 can1-100 his3-11,15::pRS303-DBF4-CDC7-pGAL1-GAL4::HIS3Mx4 pep4::hph-NT1 DBF4-3FLAG::KanMx leu2-3,112::CDC7-9myc::LEU2</i>	<i>pGAL-DBF4-3FLAG-CDC7-9myc</i>	This study

### Antibodies

Proteins were detected using specific antibodies: rabbit-anti-Dpb11 (BPF19, Pfander lab), rabbit-anti-Slx4 (2057, Pfander lab), goat-anti-Cdc5 (sc-6733, Santa Cruz), rabbit-anti-Cdc7 (Diffley lab), rabbit-anti-Clb2 (sc-9071, Santa Cruz), goat-anti-Dbf4 (sc-5705; Santa Cruz), rabbit-anti-FLAG (F7425, Sigma), mouse-anti-myc (05-724, clone 4A6; Millipore), mouse-anti-Gal4-AD (TA-C10; Santa Cruz), mouse-anti-Gal4-BD (RK5C1; Santa Cruz).

### FACS analysis

$1 \times 10^7$  -  $2 \times 10^7$  cells were harvested by centrifugation and resuspended in 70% ethanol + 50 mM Tris pH 7.8. After centrifugation cells were washed with 1 ml 50 mM Tris pH 7.8 (Tris buffer) followed by resuspending in 520  $\mu$ l RNase solution (500  $\mu$ l 50 mM Tris pH 7.8 + 20  $\mu$ l RNase A (10 mg/ml in 10 mM Tris pH 7.5, 10 mM MgCl<sub>2</sub>) and incubation for 4

h at 37 °C. Next, cells were treated with proteinase K (200 µl Tris buffer + 20 µl proteinase K (10 mg/ml in 50% glycerol, 10 mM Tris pH 7.5, 25 mM CaCl<sub>2</sub>) and incubated for 30' at 50 °C. After centrifugation cells were resuspended in 500 µl Tris buffer. Before measuring the DNA content, samples were sonified (5"; 50% CYCLE; minimum POWER) and stained by SYTOX solution (999 µl Tris buffer + 1 µl SYTOX). Measurement was performed using FL1 channel 520 for SYTOX-DNA by BD FACSCalibur system.

### **Acrylamide gel electrophoresis and western blot analysis**

Protein samples were separated by standard SDS-polyacrylamide gel electrophoresis in 4-12% Novex NuPAGE Bis-Tris precast gels (ThermoFisher) with MOPS buffer (50 mM MOPS, 50 mM Tris-base, 1.025 mM EDTA, 0.1% SDS, adjusted to pH 7.7). To resolve phosphorylation shifts of Mms4 in Fig. EV1, and of Ulp2<sup>9myc</sup> or Scc1<sup>9myc</sup> (Fig. S2E), protein samples were separated in 7% Novex NuPAGE Tris-Acetate precast gel (ThermoFisher) with Tris-Acetate buffer (50 mM Tris-base, 50 mM Tricine, 0.1% SDS, adjusted to pH 8.24).

After electrophoresis, proteins were transferred to a nitrocellulose membrane (Amersham Protran Premium 0.45 µm NC) using a tank blotting system. Membranes were incubated with primary antibodies at 4 °C overnight. Incubation with appropriate secondary antibodies coupled to horseradish peroxidase (HRP) was performed at room temperature for 3 h. Membranes were washed five times for 5 min with western wash buffer (50 mM Tris pH 7.5, 137 mM NaCl, 3 mM KCl, 0.2 % NP-40) and incubated with Pierce ECL western blotting substrate (ThermoFisher) according to the instructions of the manufacturer. Chemiluminescence was detected with a tabletop film processor (OPTMAX, Protec).

### **Yeast Two-Hybrid analysis**

The plasmids used for yeast two-hybrid analysis in this study were based on pGAD-C1 and pGBD-C1. To assay for an interaction between the proteins, respective plasmids were transformed into competent PJ69-7A cells. Transformants were spotted in serial dilution (1:5) either on SC-Leu-Trp plates (control) or on SC-Leu-Trp-His plates (selection) and incubated at 30 °C for 2-3 days. Cells from the control plates were then grown in SC-Leu-Trp to log-phase to take samples for subsequent analysis of the expression of the AD-/BD-fusion proteins by western blot.

### **Preparation of whole-cell extracts (alkaline lysis/TCA)**

Cell pellets were re-suspended in 1 ml pre-cooled H<sub>2</sub>O and incubated with 150 µl of freshly prepared lysis solution (1.85 M NaOH, 7.5% beta-mercaptoethanol) at 4 °C for 15 min. Then, the lysate was admixed with 150 µl 55% trichloroacetic acid (TCA) and incubated at 4 °C for 10 min. After centrifugation and careful aspiration of the supernatant, the precipitated proteins were re-suspended in 50 µl HU-buffer (8 M urea, 5% SDS, 200 mM Tris pH 6.8, 1.5% dithiothreitol, traces of bromophenol blue) and incubated at 65 °C for 10 min.

### **Synchronization of cells**

Logarithmic growing cells were synchronized in mitosis by nocodazole (5 µg/ml), in S-phase by HU (200 mM), or in G1-phase by  $\alpha$ -factor (5-10 µg/ml). Release from G1 synchronization into S-phase was performed by washing twice in pre-warmed YPD, and suspending cells in pre-warmed YPD with nocodazole, with HU or without chemical.

### **Drug treatment**

DNA damage in liquid cultures was induced by addition of phleomycin to a final concentration of 50 µg/ml.

For solid media, concentrations of methyl methanesulfonate (MMS) were as indicated in the figures. Cells from stationary grown ON cultures were spotted in serial dilution (1:5) and incubated at 30 °C for 2-3 days.

### **Interaction assays**

After cell growth under the indicated conditions, yeast extracts were obtained by freezer mill lysis (Spex Sample Prep) in lysis buffer (100 mM Hepes pH 7.6, 200 mM KOAc, 0.1% NP-40, 10% glycerol, 2 mM b-ME, 100 mM octadecanoic acid, 10 mM NaF, 20 mM b-glycerophosphate, 400 µM PMSF, 4 µM aprotinin, 4 mM benzamidin, 400 µM leupeptin, 300 µM pepstatin A). Co-IP was performed for 2 hours with head-over-tail rotation at 4 °C using anti-FLAG agarose resin (Sigma). Non-specific background was removed by six washes and bound proteins were eluted by incubation with 0.5 mg/ml 3X FLAG-peptide (Sigma). The TCA-precipitated eluates were resolved on 4-12% NuPAGE gradient gels (Invitrogen), and analyzed by standard Western blotting techniques.

### **SILAC-based quantitative mass-spectrometry**

For Co-IP experiments followed by mass spectrometry analysis, cells deficient in lysine biosynthesis were grown in synthetic complete (SC) medium supplemented with normal

lysine (“light” medium) or heavy-isotope-labeled lysine (Lys6 or Lys8; “heavy” medium) from Cambridge Isotope Laboratories and arrested in G2/M phase with nocodazole. In SILAC experiments with high-copy expression of *MUS81-MMS4*, overexpression was induced by addition of 2% galactose for 2 h after nocodazole arrest.

Lysates were prepared by harvesting cells in equal amounts after growth under the indicated conditions. After co-IP, eluted proteins from light and heavy cultures were pooled, TCA precipitated and separated on a 4-12% NuPAGE Bis-Tris gel (Invitrogen). The gel was stained with GelCode Blue (Thermo Scientific). The gel lane was excised into ten slices and peptides were analyzed by LC-MS/MS after in-gel Lys-C digestion. Samples were measured on an LTQ-Orbitrap and analyzed using MaxQuant (Cox & Mann, 2008).

For analysis of proteins (Fig. S1A, 2E, S2A, EV3A, 6D, S6A), log<sub>2</sub> values of H/L ratios from two label-switch experiments without ratio count cut-off were plotted against each other.

For analysis of phosphorylation sites from endogenous protein levels (Fig. 3A-B, S7A), H/L ratios for Mms4 peptides were calculated from the corresponding H and L intensities of MS evidences and plotted in their log<sub>2</sub> values against the log<sub>10</sub> values of the peptide’s overall intensity. Evidences of non-phosphorylated Mms4 peptides are shown in grey, evidences of phosphorylated peptides are shown in black. Phosphorylated peptides were sorted into categories according to their phosphorylation status. Putative DDK target sites were differentiated into the categories pSpS (red), pSS (orange) or SpS (yellow), in which the respective residues of the (S/T)(S/T) motif were phosphorylated (detected phosphorylation probability >0.7). Phosphorylated peptides matching the Cdc5 consensus site are coloured in blue. Numbers indicate the phosphorylated residue in the depicted peptide. An asterisk marks peptide evidences that contained measured intensity values exclusively in the H or L sample. Their ratio value was set to a fixed value.

For analysis of phosphorylation sites from overexpressed *MUS81-MMS4* (Fig. 3C-D, S7B), log<sub>2</sub> values of H/L ratios of Mms4 peptides were plotted against the log<sub>10</sub> values of the peptide’s intensity. Depicted are phosphorylated peptides only. Peptides were sorted into categories according to their phosphorylation status. Putative DDK target sites were differentiated into the categories pSpS (red), pSS (orange) or SpS (yellow), in which the respective residues of the (S/T)(S/T) motif were phosphorylated (detected phosphorylation probability >0.7). Phosphorylated peptides matching the Cdc5 consensus site are coloured in blue. All other phosphorylated peptides are marked in grey. Bars depict the mean of the ratios of the respective category.

## Protein purification

CDK was expressed in *E. coli* BL21 pRIL cells (Agilent). Mus81-Mms4, DDK and Cdc5 were overexpressed in *S. cerevisiae* from a galactose-inducible GAL1-10 promoter. All purification steps were performed on ice or at 4 °C.

### *Purification of Mus81-Mms4 from S. cerevisiae*

*FLAG3MUS81* and *GST-HIS10-STREP2MMS4* were cloned under the control of the *GAL1,10* bidirectional promoter in a pRS306 derivative plasmid. The resulting vector was linearized with *StuI* and integrated at the *ura3-1* locus of a W303 *pep4Δ* strain.

The resulting MGBY3294 strain was grown in YP+2% raffinose to mid-log phase at 25 °C and protein expression was induced by addition of 2% galactose. Cells (10 liters at ~2-4x10<sup>7</sup> cells/ml) were harvested, washed and resuspended in a small volume of A500 buffer (40 mM Tris-HCl pH 7.5, 500 mM NaCl, 20% glycerol, 0.1% NP-40, 1 mM DTT) containing phosphatase and protease inhibitors and mechanically disrupted. The frozen lysate was resuspended in 2 volumes of A500, cleared by ultracentrifugation and incubated with anti-FLAG M2 agarose beads (Sigma) for 1 h at 4 °C. After extensive washing of the beads in A500, Mus81-Mms4 was dephosphorylated by treatment with 10,000 units of lambda phosphatase (New England Biolabs) for 30 min at room temperature. Beads were washed in A500 buffer and Mus81-Mms4 was then eluted with 3 volumes of A500 supplemented with 0.5 mg/ml 3X FLAG-peptide (Sigma). The eluate was then adjusted to 5 mM imidazole and proteins were loaded onto a Ni-NTA column (Qiagen). The column was washed with A500 buffer containing increasing concentrations of imidazole up to 50 mM, and finally Mus81-Mms4 was eluted with A500 containing 300 mM imidazole. The eluate was dialyzed extensively against A500, and stored in aliquots at -80 °C. Protein concentrations were determined using the Bradford assay (BioRad) and on Coomassie-stained PAGE gels using BSA as the standard, which also confirmed absence of phosphorylation-dependent electrophoretic migration shifts. Control experiments confirmed the absence of non-specific endo- or exonuclease activities.

### *Purification of bacterially expressed CDK2/cycA<sup>ΔN170</sup>*

To generate CDK2/cycA<sup>ΔN170</sup> complex, *GSTCDK2* and *His6cycA<sup>ΔN170</sup>* were expressed separately. Bacteria with either expression plasmids were grown in 1 l LB medium supplemented with antibiotics to mid-log phase. Both cultures were cooled down on ice for 5 min to increase chaperone expression followed by addition of 1 mM IPTG and incubation for 20 h at 20 °C. Cells were pelleted and resuspended in 40 ml lysis buffer

(300 mM NaCl, 20 mM HEPES pH 7.6, 5 mM  $\beta$ -mercaptoethanol, 0.01% NP-40, 100  $\mu$ M AEBSF, 1x complete protease inhibitor cocktail EDTA-free) followed by lysis with an EmulsiFlex-C3 system for three rounds at 1,000 bar. Cell debris was spun down at 140,000 g for 45 min. To allow complex formation between both subunits, extracts were pooled and incubated for 45 min. For glutathione affinity chromatography, 1 ml bed volume of equilibrated Glutathione Sepharose beads were added to the extract and incubated for 2 h. Beads were then washed four times with 25 CV Wash Buffer B2 (300 mM NaCl, 20 mM HEPES pH 7.6, 5 mM  $\beta$ -mercaptoethanol, 0.01% NP-40) before elution was achieved by protease cleavage. For this purpose, beads were resuspended in 1 CV wash buffer (150 mM NaCl, 20 mM HEPES pH 7.6, 5 mM  $\beta$ -mercaptoethanol, 0.01% NP-40) and incubated together with 250 U GST-PreScission protease (MPIB Core Facility) for 18 h. The eluate was then adjusted to 300 mM NaCl and 6 mM imidazole for subsequent Ni-NTA affinity chromatography. Here, a bed volume of 1 ml equilibrated Ni-NTA Agarose (Qiagen) was added to the eluate and incubated for 1 h. Beads were subsequently washed four times with 15 CV wash buffer (300 mM NaCl) + 6 mM imidazole and five times with 2 CV wash buffer (300 mM NaCl) + 6 mM imidazole + 5% glycerol. Elution was then performed with wash buffer (300 mM NaCl) + 250 mM imidazole. Fractions containing CDK were pooled and dialyzed by stirring two times against 300 volumes of dialysis buffer (150 mM NaCl, 50 mM HEPES pH 7.6, 0.1% NP-40, 2 mM  $\beta$ -mercaptoethanol, 10% glycerol) for 4 h in a Slide-A-Lyzer Dialysis Cassette (Thermo Scientific). Dialysed material was recovered, aliquoted, snap-frozen and stored at -80 °C.

#### *Purification of Cdc5 from S. cerevisiae*

YFZ020 was grown in 10 l YP medium + 2% raffinose at 30 °C until mid-log phase before expression was induced by addition of 2% galactose. After 4 h of induction, yeast cells were harvested and washed twice with 250 ml 1 M Sorbitol + 25 mM HEPES pH 7.6. The pellet was resuspended in 1 volume of lysis buffer (500 mM NaCl, 100 mM HEPES pH 7.6, 0.1% NP-40, 10% glycerol, 2 mM  $\beta$ -mercaptoethanol, 400  $\mu$ M PMSF, 4  $\mu$ M aprotinin, 4 mM benzamidin, 400  $\mu$ M leupeptin, 300  $\mu$ M pepstatin A, 4x complete protease inhibitor cocktail, EDTA-free) and frozen drop-wise in liquid nitrogen. Frozen cell drops were crushed using a freezer/mill system (Spex Sample Prep). Cell powder was thawed on ice and centrifuged at >185,000 g for 1 h. The clear phase was recovered and incubated with 1 ml bed volume of anti-FLAG M2 resin (Sigma) equilibrated in lysis buffer. After 2 h of incubation, the resin was washed five times with 10 CV of wash buffer (500 mM NaCl, 100 mM HEPES pH 7.6, 0.1% NP-40, 10% glycerol, 2 mM  $\beta$ -

mercaptoethanol). Two elution steps were performed by adding 1 CV 0.5 mg/mL 3FLAG peptide in wash buffer and incubation for 30 min. Obtained fractions were pooled, brought to a conductivity of 10 mS/cm (100 mM salt) and subjected to anion exchange chromatography using a MonoQ 5/50 GL column with a salt gradient of 0.1-1 M NaCl over 20 CV. Cdc5<sup>3FLAG</sup> eluted at a conductivity of ~15 mS/cm. Kinase containing fractions were aliquoted, snap-frozen and stored at -80 °C.

#### *Purification of DDK from S. cerevisiae*

DDK was purified as described by Gros *et al.* with modifications (Gros *et al.* 2014). YFZ021 cells were grown in 10 l YP medium + 2% raffinose at 30 °C until mid-log phase before expression was induced by addition of 2% galactose. After 4 h of incubation, yeast cells were harvested and washed twice with 250 ml 1 M Sorbitol + 25 mM HEPES pH 7.6. The pellet was resuspended in 1 volume of lysis buffer (400 mM NaCl, 100 mM HEPES pH 7.6, 0.1% NP-40, 10% glycerol, 2 mM  $\beta$ -mercaptoethanol, 400  $\mu$ M PMSF, 4  $\mu$ M aprotinin, 4 mM benzamidin, 400  $\mu$ M leupeptin, 300  $\mu$ M pepstatin A, 4x complete protease inhibitor cocktail EDTA-free) and frozen drop-wise in liquid nitrogen. Frozen cell drops were crushed using a freezer/mill system. Cell powder was thawed on ice and centrifuged at >185,000 g for 1 h. The clear phase was recovered and incubated with 1 ml bed volume of anti-FLAG M2 resin (equilibrated in lysis buffer). After incubation for 2 h at 4 °C, the resin was washed six times with 2 CV wash buffer (400 mM NaCl, 100 mM HEPES pH 7.6, 0.1% NP-40, 10% glycerol, 2 mM  $\beta$ -mercaptoethanol). For  $\lambda$ -phosphatase treatment, beads were resuspended in 1 CV wash buffer + 2 mM MnCl<sub>2</sub> + 900 U  $\lambda$ -phosphatase (New England Biolabs) and incubated for 1 h at 30 °C in a tabletop thermoshaker. Beads were recovered and bound DDK was eluted twice with 1 CV 0.5 mg/ml 3FLAG peptide in wash buffer for 30 min. Elutions were pooled, concentrated using a Vivaspin 500 MWCO 50.000 (GE healthcare) and fractionated by size exclusion chromatography using a Superdex 200 GL 10/300 column (GE healthcare, equilibrated in wash buffer) over 1.2 CV. DDK containing fractions were pooled, brought to a conductivity of 10 mS/cm (100 mM salt) and fractionated by anion exchange chromatography using a MonoQ 5/50 GL column with a salt gradient of 0.1-1 M NaCl over 20 CV. DDK containing fractions eluted at ~24-26 mS/cm and were aliquoted, snap frozen and stored at -80 °C.

## ***In vitro* kinase assays**

### *Sequential kinase assays with purified Mus81-Mms4*

Kinase assays were performed as described previously (Pfander & Diffley, 2011; Mordes *et al.*, 2008) with minor modifications.

Per reaction 20 pmol Mus81-Mms4 were used as substrate for 10 pmol kinase (CDK2/cyclinA<sup>ΔN170</sup>, DDK and/or Cdc5) in a 50 μL reaction volume containing 5 μg BSA. For sequential phosphorylation reactions Mus81-Mms4 was immobilized to Glutathione Sepharose 4B resin (GE Healthcare) for 1 h at 4 °C shaking. Beads were washed twice with binding buffer-100 (100 mM Hepes pH 7.6, 100 mM KOAc, 10% glycerol, 0.02% NP-40, 2 mM β-mercaptoethanol) and once with kinase buffer (10 mM HEPES pH 7.6, 100 mM KOAc, 50 mM β-glycerophosphate, 10 mM MgCl<sub>2</sub>, 2 mM β-mercaptoethanol), and aliquoted. Residual buffer was removed.

Priming phosphorylation reactions were performed by addition of 10 pmol (of each) kinase and started by addition of 2 or 10 mM (Fig. 1B, S1C) ATP. For samples without priming reaction the equivalent volume of added kinase was substituted by kinase buffer. After 30 min at 30 °C in a tabletop shaker beads were washed twice with binding buffer-200 (100 mM Hepes pH 7.6, 200 mM KOAc, 10% glycerol, 0.02% NP-40, 2 mM β-mercaptoethanol), once with binding buffer-100 and once with kinase buffer.

The consecutive kinase reaction was performed by addition of 10 pmol kinase and started by addition of 1 mM ATP + 5 μCi γ[<sup>32</sup>P]-ATP (PerkinElmer). After incubation for 30 min shaking at 30 °C reactions were stopped by addition of Laemmli sample buffer followed by boiling at 95 °C.

For kinetic analysis of the phosphorylation reactions (Fig. S1C), the second kinase reaction was upscaled to 100 μl and 20 μl samples were taken at indicated time points. Proteins were separated on NuPAGE Novex 12% Bis-Tris gels (ThermoFisher) and analyzed by autoradiography using a Typhoon FLA 9500 imager (GE healthcare).

### *Kinase assays using synthetic Mms4 peptides*

Kinase reactions were performed with 25 μg desthiobiotin-labelled Mms4 peptide and 10 pmol kinase in kinase buffer (10 mM HEPES pH 7.6, 10 mM β-glycerophosphate, 10 mM MgCl<sub>2</sub>, 5 mM Mg(OAc)<sub>2</sub>, 2 mM β-mercaptoethanol) with 100 mM KOAc in a 50 μL reaction volume containing 5 μg BSA. Reactions were started by addition of 1 mM ATP + 5 μCi γ[<sup>32</sup>P]-ATP. After incubation for 30 min shaking at 30 °C reactions were stopped by addition of Laemmli sample buffer followed by boiling at 95 °C. Proteins were separated on NuPAGE Novex 12% Bis-Tris gels (ThermoFisher) in MES buffer and analyzed by autoradiography using a Typhoon FLA 9500 imager (GE healthcare).

### **Nuclease assays**

5'-Cy3-end-labelled oligonucleotides were used to prepare synthetic nicked Holliday Junctions (nHJ) as described (Rass & West, 2008). Nuclease assays were carried out with immunopurified Mus81<sup>9myc</sup> or Mus81<sup>3FLAG</sup> (Fig. S4A) from cells arrested in mitosis with nocodazole. The anti-myc/anti-FLAG immunoprecipitates were extensively washed and mixed with 10 µl reaction buffer (50 mM Tris-HCl pH 7.5, 3 mM MgCl<sub>2</sub>) containing 30 ng 5'-Cy3-end-labelled nHJs or RFs <sup>11</sup>. Reactions were incubated for the indicated times with gentle rotation at 30 °C and stopped by addition of 5 µl 10 mg/ml proteinase K and 2% SDS, and further incubation at 37 °C for 1 h. Loading buffer was added and fluorophore-labelled products were separated by 10% PAGE, and analyzed using a Typhoon scanner. Substrate cleavage was normalized using the level of immunoprecipitated Mus81<sup>9myc</sup> as reference.

### **DSB-induced recombination assay**

The DSB-induced recombination assay was performed as described previously (Ho *et al.*, 2010). In brief, diploids were grown in liquid YPAR (YPR + 40 mg/l Adenine) until the cultures reached an OD<sub>600</sub> of 0.5. Cells were arrested with nocodazole and I-SceI expression was induced by adding galactose to a final concentration of 2%. After 2.5 h cells were plated onto YPAD (YPD + 10 mg/l Adenine), incubated for 3-4 days and then replica plated onto YPAD+Hyg+Nat, YPAD+Hyg, YPAD+Nat, SC-Met, SC-Ura, and SCR-ADE+Gal media to classify recombination events. The different classes depicted arise from repair of DSBs by either short tract or long tract gene conversion which produces ade2-n or ADE+ recombinants, respectively (white class: two short tract conversions; red class: two long tract conversions; red/white class: one short and one long tract conversion). Within the distinct classes CO events are measured by the number of colonies that have rendered both daughter cells homozygous for the HPH and NAT marker.

## Appendix References

- Cox J & Mann M (2008) MaxQuant enables high peptide identification rates, individualized p.p.b.-range mass accuracies and proteome-wide protein quantification. *Nat Biotechnol* **26**(12): 1367-1372
- Gritenaite D, Princz LN, Szakal B, Bantele SCS, Wendeler L, Schilbach S, Habermann BH, Matos J, Lisby M, Branzei D & Pfander B (2014) A cell cycle-regulated Slx4-Dpb11 complex promotes the resolution of DNA repair intermediates linked to stalled replication. *Genes Dev* **28**: 1604–1619
- Gros J, Devbhandari S & Remus D (2014) Origin plasticity during budding yeast DNA replication *in vitro*. *EMBO J* **33**(6): 621-636
- Ho CK, Mazón G, Lam AF & Symington LS (2010) Mus81 and Yen1 promote reciprocal exchange during mitotic recombination to maintain genome integrity in budding yeast. *Mol Cell* **40**: 988–1000
- James P, Halladay J & Craig EA (1996) Genomic libraries and a host strain designed for highly efficient two-hybrid selection in yeast. *Genetics* **144**: 1425-1436
- Knop M, Siegers K, Pereira G, Zachariae W, Winsor B, Nasmyth K & Schiebel E (1999) Epitope Tagging of Yeast Genes using a PCR-based Strategy: More Tags and Improved Practical Routines. *Yeast* **15**: 963-972
- Mordes DA, Nam EA & Cortez D (2008) Dpb11 activated the Mec1-Ddc2 complex. *Proc Natl Acad Sci U S A* **105**(48): 18730-18734
- Pfander B & Diffley JFX (2011) Dpb11 coordinates Mec1 kinase activation with cell cycle-regulated Rad9 recruitment. *EMBO J*. **30**: 4897–4907
- Rass U & West SC (2006) Synthetic junctions as tools to identify and characterise Holliday junction resolvases. *Meth Enzymol* **408**: 485-501
- Thomas BJ & Rothstein R (1989) Elevated recombination rates in transcriptionally active DNA. *Cell* **56**: 619-630